Five-Brane Webs, Higgs Branches and Unitary/Orthosymplectic Magnetic Quivers

M. Akhond

Department of Physics, Swansea University, Singleton Park, Swansea, UK

F. Carta

Deutsches Elektronen-Synchrotron DESY, Hamburg

S. Dwivedi

*Center for Theoretical Physics, College of Physical Science and Technology,
Sichuan University, Chengdu, China*

H. Hayashi

*Department of Physics, School of Science, Tokai University, Kitakaname,
Hiratsuka-shi, Kanagawa, Japan*

S.-S. Kim

*School of Physics, University of Electronic Science and Technology of China,
Chengdu, Sichuan, China*

F. Yagi

*School of Mathematics, Southwest Jiaotong University,
Chengdu, Sichuan, China*

Five-brane webs, Higgs branches and unitary/orthosymplectic magnetic quivers

Mohammad Akhond,[a] **Federico Carta,**[b] **Siddharth Dwivedi,**[c] **Hirotaka Hayashi,**[d] **Sung-Soo Kim,**[e] **and Futoshi Yagi**[f]

[a]*Department of Physics, Swansea University,*
Singleton Park, Swansea, SA2 8PP, U.K.

[b]*Deutches Electronen-Synchrotron, DESY,*
Notkestraße 85, 22607 Hamburg, Germany

[c]*Center for Theoretical Physics, College of Physical Science and Technology, Sichuan University,*
Chengdu, 610064, China

[d]*Department of Physics, School of Science, Tokai University,*
4-1-1 Kitakaname, Hiratsuka-shi, Kanagawa 259-1292, Japan

[e]*School of Physics, University of Electronic Science and Technology of China,*
No.4, Section 2, North Jianshe Road, Chengdu, Sichuan 610054, China

[f]*School of Mathematics, Southwest Jiaotong University,*
West zone, High-tech district, Chengdu, Sichuan 611756, China

E-mail: akhondmohammad@gmail.com, federico.carta@desy.de,
sdwivedi@scu.edu.cn, h.hayashi@tokai.ac.jp, sungsoo.kim@uestc.edu.cn,
futoshi_yagi@swjtu.edu.cn

ABSTRACT: We study the Higgs branch of 5d superconformal theories engineered from brane webs with orientifold five-planes. We propose a generalization of the rules to derive magnetic quivers from brane webs pioneered in [1], by analyzing theories that can be described with a brane web with and without O5 planes. Our proposed magnetic quivers include novel features, such as hypermultiplets transforming in the fundamental-fundamental representation of two gauge nodes, antisymmetric matter, and $\mathbb{Z}_2$ gauge nodes. We test our results by computing the Coulomb and Higgs branch Hilbert series of the magnetic quivers obtained from the two distinct constructions and find agreement in all cases.

Contents

1 Introduction

It has been known for some time that there are interacting UV fixed points of the renormalization group (RG) in five dimensions [2–4]. Many of these superconformal theories (SCFTs) admit a relevant deformation whose low energy dynamics is captured effectively by an $\mathcal{N} = 1$ gauge theory, despite the fact that Yang-Mills (YM) interactions are power-counting non-renormalizable in five dimensions. A generic feature of such an RG flow is that the global symmetries of the fixed point theory are enhanced with respect to the manifest global symmetries of the gauge theory description, which has been confirmed by various observables such as superconformal indices, Nekrasov partition functions and topological vertex [5–24]. It was also argued from the presence of instanton operators [25–29], defined as defect operators, that have the charges associated with the topological current $J_I = \frac{1}{8\pi^2}\text{Tr} * (F \wedge F)$. This current can mix with the flavour symmetries in the UV to form a larger symmetry group. In the case of a quiver gauge theory, there are as many topological currents as the number of gauge nodes. Their algebra may be promoted to a non-abelian one, often without mixing with flavour symmetries.

The 5-dimensional (5d) $\mathcal{N} = 1$ gauge theories admit an embedding into type IIB string theory which is realized as 5-brane webs [30, 31]. The 5-brane webs have been a powerful tool to study 5d SCFTs, as they not only provides an effective description of the SCFT at low energy, but also reveal rich non-perturbative aspects of the SCFTs such as global symmetry enhancement [32–34] and various dualities including S-duality as well as novel UV-dualities [11, 12, 14, 21, 23, 24, 35–39].

Of particular significance to this story is the Higgs branch of the moduli space of the 5d theory. The Higgs branch is both sensitive to the symmetry enhancement and computable at all values of the YM coupling. It also undergoes other dramatic effects along the flow, such as the appearance of new flat directions at the UV fixed point.

A program to study Higgs branches of 5d theories by relating them to Coulomb branches of 3d $\mathcal{N} = 4$ quiver gauge theories, henceforth referred to as *magnetic quivers*, was initiated in [40, 41], following earlier work [42, 43] observing similar connections. For related work on magnetic quivers, also see [44]. 5-brane webs also play an important role in constructing the 3d quiver gauge theories associated to the Higgs branch. A set of rules were established in [45, 46] to derive the magnetic quivers directly from the 5-brane web. In particular, the stable intersection number from the substructure of the 5-brane web at the Higgs branch captures the multiplicity of edges connecting nodes of the 3d quiver [45]. This was later extended to brane webs with O5-planes in [1].

In this paper we continue along this line of logic. We generalize the construction of magnetic quivers from O5-planes by adding new entries to the list of rules established in [1]. We examine theories that can be constructed both using ordinary brane webs, as well as brane webs with O5-planes. We verify the equivalence of the Coulomb branch of the magnetic quivers obtained from the two distinct constructions by a Hilbert series computation. We view the agreement in these computations as a non-trivial test of our conjectured rules. We organize our study according to the asymptotics of the brane configuration. It will be convenient to distinguish configurations by the asymptotic charges of the O5-plane.

Within a given set of asymptotic O5-plane charges, we further divide theories according to (p, q) charges of the asymptotic 5-branes. We use naming conventions for the various cases inspired by [47]. Our new rules translate to appearance of new qualitative features in the magnetic quivers. This includes exotic bifundamental matter and matter in the 2nd rank tensor representations. Our rules are obtained by examining several 5d theories which can be constructed both using a brane web with an O5-plane as well as brane web without the orientifold. We achieve this by considering 5d Orthosymplectic (OSp) quivers with an S-dual description as $D_3 = A_3$ type Dynkin quiver. Upon identifying deformation parameters of the ordinary web description with those of the orientifold web one can produce many daughter theories by deforming the two sides in an equivalent way. After the deformation the unitary webs may or may not admit a simple gauge theory description, though this is not important for our purposes. We can then derive magnetic quivers for the unitary web constructions following [45], which serve as a consistency check of our conjectured rules for the OSp magnetic quivers obtained from orientifold webs.

Although the original motivations for this work are as above, our study also hints towards implications for the magnetic quivers, viewed as 3d $\mathcal{N} = 4$ gauge theories. In order to verify our results we performed Hilbert series computations for both the Coulomb and Higgs branches of these theories. In all cases we found an agreement between the two computations. Together with the fact that the 5d origin of these theories is identical, one is tempted to conjecture that the two theories are dual as 3d $\mathcal{N} = 4$ theories. However our analysis here is too simple to determine exactly in which sense the two theories are dual to each other.

The organization of the paper is as follows. We divide the content by asymptotic behavior of orientifold planes. In section 2 we start from examples which come from 5-brane web diagrams with asymptotic $O5^-$-planes on both ends and obtain magnetic quivers from the configurations. In the course of obtaining the magnetic quivers we observe new rules. We will also compute the Hilbert series of Coulomb branches of these magnetic quivers and compare them with those which arise from ordinary web diagrams. Section 3 considers cases where the configurations have $O5^+$-planes on both ends, and section 4 considers examples with an $O5^-$-plane on one end and an $O5^+$-plane on the other end. In section 5, we consider some cases which involve an $\widetilde{O5}^+$-plane in the diagrams. Finally we summarise our conclusions together with a set of open problems that we find are worth further investigation in section 6. Appendix A summarizes the method for computing the Hilbert series of Coulomb branches and Higgs branches. Appendix B gives some details of the Coulomb branch Hilbert series in the main sections. In appendix C we give more support for the rule about the number of charge 2 hypermultiplets given in section 2. Appendix D summarizes more examples from brane configurations with $O5^-$-planes on both ends.

Notation. To avoid the cluttering of the quiver diagrams, we will use a color coding to represent the unitary and orthosymplectic nodes as given below:

Node type	U(n)	SO(m)	USp($2k$)
Gauge	○ n	● m	● $2k$
Flavor	□ n	■ m	■ $2k$

. $\qquad$ (1.1)

In the above, the circular nodes denote the gauge group while the square nodes represent a global (rather than gauge) symmetry group. In this work, we will have three kinds of links connecting the nodes: solid line, dashed line and wavy line. These links transform under the representations of the nodes it connects with the following dictionary.

Link type	Interpretation
○——○	hypermultiplet transforming in the bifundamental representation
○——●	hypermultiplet transforming in the bifundamental representation
○——●	hypermultiplet transforming in the bifundamental representation
●——●	half-hypermultiplet transforming in the bifundamental representation
○----○	hypermultiplet in the fundamental-fundamental representation
○〰〰□	charge 2 hypermultiplet

(1.2)

In order to avoid confusion, we will denote 5d (electric) quivers as $\cdots - G - G_j - \cdots$ and use square braces $[F]$ to denote flavor nodes.

2 Magnetic quivers from O5$^-$ - O5$^-$

We first consider examples whose brane configurations are accompanied with two asymptotic O5$^-$-planes.
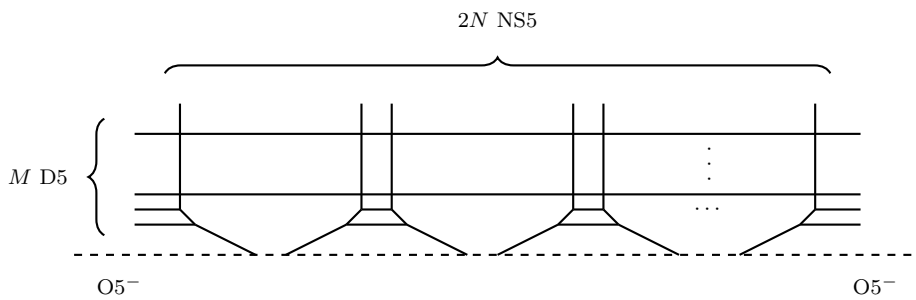
2.1 The $\#_{M,N}$ theory

Figure 1: 5-brane web for the $\#_{M,N}$ theory.

The first example we consider is the brane configuration obtained by intersecting M D5 and $2N$ NS5 branes on top of an O5-plane, which in this section we take to be asymptotically an O5$^-$-plane. We call the theory on the web the $\#_{M,N}$ theory. The brane web for

this theory is depicted in Figure 1. The effective theory on the Coulomb branch is a linear orthosymplectic quiver

$$\overbrace{[M] - \mathrm{USp}(2M - 4) - \mathrm{SO}(2M) - \mathrm{USp}(2M - 4) - \cdots - \mathrm{SO}(2M) - \mathrm{USp}(2M - 4)}^{2N - 1} - [M] \tag{2.1}$$

The corresponding magnetic quiver was in fact already derived in [1]. We will not repeat the steps here and simply recall that it is given by

$$(2.2)$$

The 5d theory admits an S-dual description, as a D-type Dynkin quiver of special-unitary nodes [38, 48]. In the special case when $M = 3$, the S-dual theory on the Coulomb branch is

$$\begin{array}{c} [2N] \\ | \\ \mathrm{SU}(N) - \mathrm{SU}(2N) - \mathrm{SU}(N) \end{array} \tag{2.3}$$

which can also be engineered via an ordinary web diagram, without an O5-plane. One way to see this is to consider gluing together N copies of $\mathrm{USp}(2) + 6\mathbf{F}$, by successive gauging $\mathfrak{so}(6)$ subalgebra of the flavour symmetry. This should be equivalent to gluing together N copies of $\mathrm{SU}(2) + 6\mathbf{F}$ by gauging $\mathfrak{su}(4)$ subalgebra of the global symmetry. Then we perform S-duality and the diagram yields the theory in (2.3). See Figure 2 for the $N = 2$ example. We will make use of this construction to obtain web diagrams without O5-planes. Furthermore there are various ways to realize $\mathrm{USp}(2)$ gauge theory with six flavors depending on how we attach flavors to the diagram. Depending on situations we will use useful diagrams of $\mathrm{SU}(2) + 6\mathbf{F}$ for the $\mathfrak{su}(4)$ gauging. The unitary web diagram for the $\#_{3,N}$ theory is shown in the Figure 3.

Given this diagram, we can immediately obtain the magnetic quiver using the rules in [45]. We are thus led to claim the equivalence of the Coulomb branch of (2.2), for $M = 3$ with the following unitary magnetic quiver.
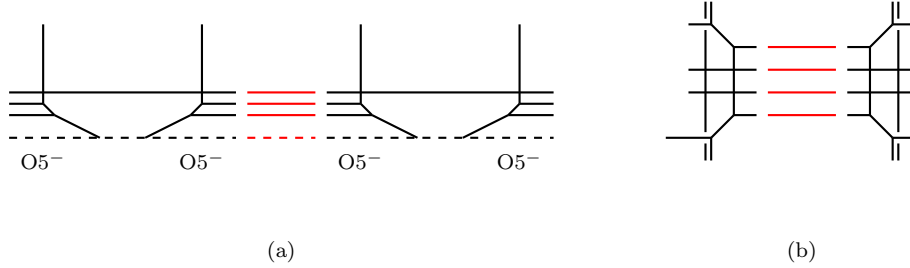

$$(2.4)$$

Figure 2: (a) Gluing together 2 copies of $\mathrm{USp}(2) + 6\mathbf{F}$ by gauging a common $\mathfrak{so}(6)$ subalgebra of their global symmetry. (b) Gluing together 2 copies of $\mathrm{SU}(2)+6\mathbf{F}$ by gauging a common $\mathfrak{su}(4)$ subalgebra of their global symmetry.
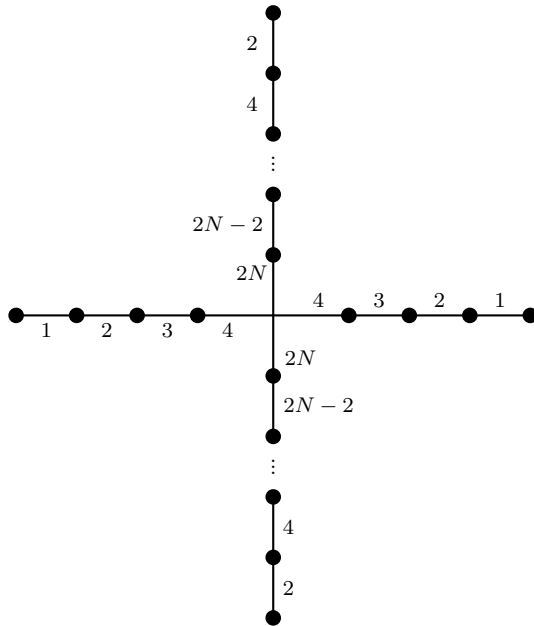

Figure 3: A unitary web realization of the $\#_{3,N}$ theory. We depict here the web at the fixed point. Black dots represent 7-branes.

Both (2.4) and the $M = 3$ case of (2.2) hint at an enhanced $\mathrm{SU}(2N) \times \mathrm{SU}(4)^2$ flavour symmetry, which can be read off from the balanced nodes [49][1]. The Coulomb and Higgs branch dimension of both quivers are also in agreement. A further non-trivial check of our discussion is the agreement of the Hilbert series, which we have explicitly computed for low values of N. For $N = 1$, the unitary magnetic quiver in (2.4) is well known with the Coulomb branch having E_7 as the enhanced global symmetry. We have tabulated the Coulomb branch Hilbert series for the unitary and the orthosymplectic magnetic quivers

---

[1]We recall the balance condition for $\mathrm{U}(r)$, $\mathrm{USp}(2r)$ and $\mathrm{SO}(m)$ is $n_f = 2r$, $n_f = 2r + 1$ and $n_f = m - 1$ respectively where n_f is the number of effective flavors. From [49], chain of p balanced alternating orthosymplectic nodes give rise to an $\mathrm{SO}(p+1)$ isometry on the CB, which is further enhanced to $\mathrm{SO}(p+2)$ if there is an $\mathrm{SO}(2)$ node at the end of the chain. A set of p balanced unitary nodes which form an ADE Dynkin diagram give rise to a symmetry of the corresponding type.

derived from the unitary and orientifold webs of $\#_{3,N}$ theory in Table 1 for some small values of N. Note that the Hilbert series for $N = 1$ is already known ([50, 51]).

$\#_{3,N}$	Unitary magnetic quiver $\mathrm{HS}(t)$	Orthosymplectic magnetic quiver	
		$\mathrm{HS}(t; \vec{m} \in \mathbb{Z})$	$\mathrm{HS}(t; \vec{m} \in \mathbb{Z} + \frac{1}{2})$
$\#_{3,1}$	$\dfrac{(1+t)\,P_0(t)}{(1-t)^{34}}$ $= 1 + 133t + 7371t^2$ $+238602t^3 + 5248750t^4$ $+85709988t^5 + \cdots$	$\dfrac{P_1(t)}{(1-t)^{34}\,(1+t)^{17}}$ $= 1 + 69t + 3723t^2 + 119434t^3$ $+2625390t^4 + 42857892t^5 + \cdots$	$\dfrac{P_2(t)}{(1-t)^{34}\,(1+t)^{17}}$ $= 64t + 3648t^2 + 119168t^3$ $+2623360t^4 + 42852096t^5 + \cdots$
$\#_{3,2}$	$1 + 45t + 1277t^2 + 27399t^3 +$ $476864t^4 + 6979468t^5 +$ $87938113t^6 + \cdots$	$1 + 45t + 1085t^2 + 18951t^3 +$ $280320t^4 + 3739084t^5 +$ $45180033t^6 + \cdots$	$192t^2 + 8448t^3 + 196544t^4 +$ $3240384t^5 + 42758080t^6 + \cdots$

Table 1: Coulomb branch Hilbert series of the unitary and orthosymplectic magnetic quivers for the $\#_{3,N}$ theory. The corresponding quivers are given in (2.4) and (2.2) respectively. For orthosymplectic quivers, we need to add the contributions of both integer and half integer fluxes. The explicit forms of the numerators $P_0(t), P_1(t), P_2(t)$ are provided in Appendix B.

2.2   The K_N family

Decoupling flavors from, say, the rightmost gauge node in the $\#_{3,N}$ theory (2.1), we obtain a family of theories which we denote by K_N^p, where p denotes the number of decoupled flavors. This family enjoys an IR quiver description as

$$\overbrace{[3] - \mathrm{USp}(2) - \mathrm{SO}(6) - \mathrm{USp}(2) - \cdots - \mathrm{SO}(6) - \mathrm{USp}(2)}^{2N-1} - [3-p] \tag{2.5}$$

Once again, it is possible to write down an ordinary web diagram for this theory, following a gluing procedure similar to Figure 2.[2] We present the orientifold and the unitary web diagrams for the family K_N^p for various number of decoupled flavors which can be found in the figures mentioned below.

Theory	Orientifold web	Unitary web
K_N^1	Figure 4	Figure 5
K_N^2	Figure 6	Figure 7
K_N^3	Figure 8	Figure 9

---

[2]The cautious reader may be concerned about the non-uniqueness of this gauging procedure which is related to the Chern-Simons level of the gauging. One can remove the ambiguity by demanding that the OSp magnetic quiver agrees with the unitary quiver obtained from the unitary web after gauging. It is also possible to reproduce the same unitary web more rigorously by identifying the map between the deformation parameters in the orientifold and unitary web of the $\#_{3,N}$ theory.

Here, we note that these are not the only possible subdivisions. We list some examples of subdivisions and their corresponding magnetic quivers. In this paper, our focus is on extracting the rules rather than an exhaustive analysis of the Higgs branch, so we consider some of the Higgs branches rather than exhausting all the branches.[3]

For reading off the magnetic quivers from the unitary web diagrams in Figures 5, 7, 9, we can use the rules established in [45]. For the magnetic quivers originated from the orientifold web diagrams in Figures 4, 6, 8, a large part of the magnetic quivers can be obtained by the rules in [1], but in fact, some part already requires an extension of the rule. In [1], it has been argued that a subweb associated with a U(1) gauge node in a magnetic quiver which passes through the O5$^-$-plane may have charge 2 hypermultiplets coupled to the U(1). Such a subweb appears in the K_N^p ($p = 1, 2, 3$) family at the center of the junction in the orientifold diagrams, and it is depicted as the subweb in black in each maximal subdivision in Figures 4, 6, 8.

The subweb configuration of the maximal subdivision in Figure 4 has already appeared in [1], for example, for the magnetic quiver of the rank-1 E_6 theory. In this case, the number of the charge 2 hypermultiplets attached to the U(1) node is zero. For the subweb configurations of the K_N^2 and K_N^3 theories, we find that the number of the charge 2 hypermultiplets is zero and one respectively to match the Coulomb branch Hilbert series for their magnetic quiver theories with the Coulomb branch Hilbert series for the corresponding unitary magnetic quivers. Based on these examples as well as the other examples which we will see later, we observe that the number of the charge 2 hypermultiplets may be counted by

$$\frac{\text{SI of subweb with its own mirror image}}{2} - \text{SI of subweb with O5}^-, \qquad (2.6)$$

where SI represents the stable intersection number discussed in [45].[4]

Let us then illustrate how the rule (2.6) works for the subwebs of the K_N^2 and K_N^3 theories. From the maximal subdivision in Figure 6, the subweb in black at the center of the junction yields a U(1) gauge node. The stable intersection number of the subweb with its own mirror image is given by

$$\text{SI of subweb with its own mirror image} = 4 - 2 = 2. \qquad (2.7)$$

On the other hand, the stable intersection number of the subweb with O5 needs some care. The subweb configuration with the orientifold is depicted in (2.8).

$$(2.8)$$

---
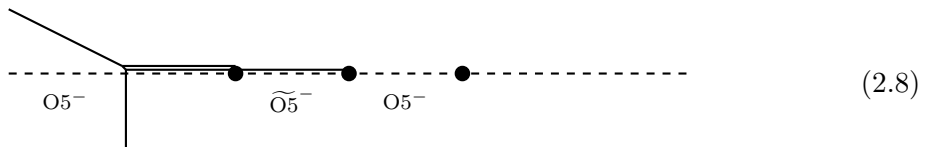
[3]We thank the authors of [52] for informing us that they were able to find some missing cones using their computer program.

[4]In this paper, we use "SI" to denote the generalized stable intersection number, which includes the contribution from the common 7-branes, for simplicity. We call usual stable intersection without the contribution from the common 7-branes as "bare SI".

Note here that the RR charge of O5$^-$-plane is -1 and that of $\widetilde{\text{O5}}^-$-plane is $-\frac{1}{2}$ due to the half D5-brane. Then the stable intersection number of the subweb with the O5-planes becomes

$$\text{SI of subweb with O5}^- = (1-1) + \left(\frac{1}{2} - \frac{1}{2}\right) + 1 = 1 \tag{2.9}$$

The first bracket in (2.9) is the stable intersection number between the left O5$^-$-plane and the subweb in (2.8), the second bracket in (2.9) is the stable intersection number between the left $\widetilde{\text{O5}}^-$-plane and the subweb in (2.8), and the last 1 is the stable intersection number between the right O5$^-$-plane and the subweb in (2.8). Namely we consider the net contribution of the stable intersection numbers between the subweb and each piece of the orientifold. Putting together the result of (2.7) and (2.9), the (2.6) becomes
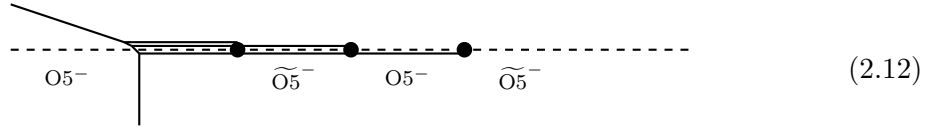
$$\frac{2}{2} - 1 = 0, \tag{2.10}$$

which is the right number of the charge 2 hypermultiplet coupled to the $U(1)$ gauge node associated to the subweb in (2.8).

We can also do the same computation for the subweb in the maximal subdivision at the center of the junction in the K_N^3 theory depicted in Figure 8. The stable intersection number of the subweb with its own mirror is given by

$$\text{SI of subweb with its own mirror image} = 6 - 3 = 3. \tag{2.11}$$

For computing the stable intersection number of the subweb with O5$^-$, we consider the configuration around the subweb depicted in (2.12).

$$\tag{2.12}$$

Then the stable intersection number of the subweb with the O5$^-$-planes becomes

$$\text{SI of subweb with O5}^- = (1-1) + \left(\frac{1}{2} - \frac{1}{2}\right) + (1-1) + \frac{1}{2} = \frac{1}{2}. \tag{2.13}$$

Hence the number of the charge 2 hypermultiplets counted by (2.6) is

$$\frac{3}{2} - \frac{1}{2} = 1, \tag{2.14}$$

which is the correct number for the charge 2 hypermultiplets coupled to the U(1) gauge node associated to the subweb in (2.12). The rule (2.6) also works for the subweb in the maximal subdivision at the center of the junction in the K_N^1 theory depicted in Figure 4.

The other parts of the magnetic quivers can be obtained from the rules established in [1, 45]. We summarize the unitary and the orthosymplectic magnetic quiver theories derived from the unitary and the orientifold web diagrams of K_N^p ($p = 1, 2, 3$) family in the Table 2. It is possible to compute the Coulomb branch Hilbert series for these magnetic quivers for each family in Table 2. We present some results in Table 3, and we see that the Hilbert series of the unitary and orthosymplectic quivers agree with each other.

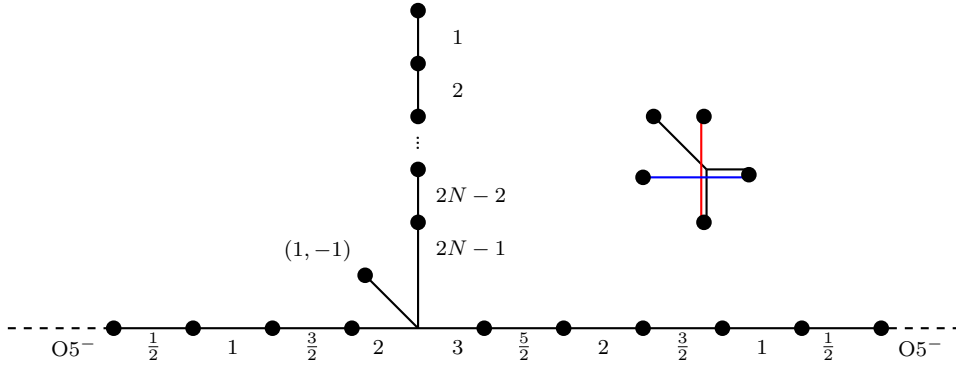**Figure 4**: An orientifold web for the K_N^1 theory and the maximal subdivision at the centre of the junction.
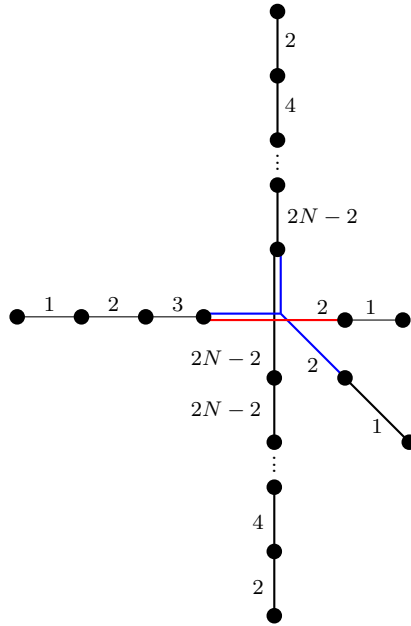

Figure 5: A unitary web for the K_N^1 theory. The maximal subdivision leading to the magnetic quiver is indicated by use of colours.

Figure 6: An orientifold web for the K_N^2 theory and the maximal subdivision at the centre of the junction.

Figure 7: A unitary web description for the K_N^2 theory, together with the maximal subdivision for the Higgs branch at infinite coupling.
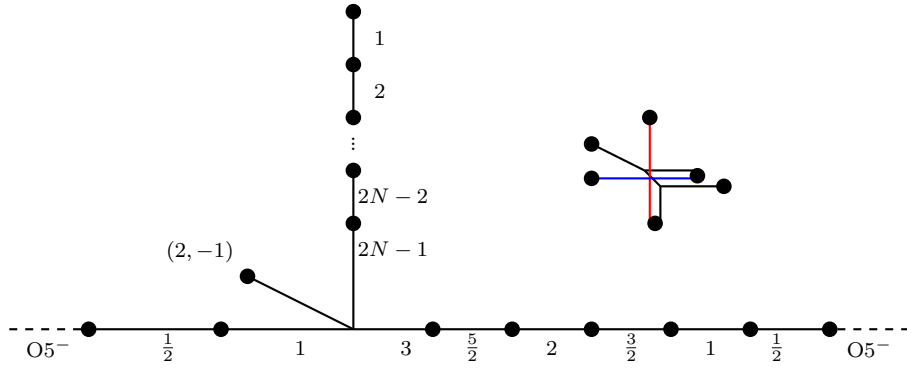

Figure 8: An orientifold web for the K_N^3 theory and the maximal subdivision at the centre of the junction.

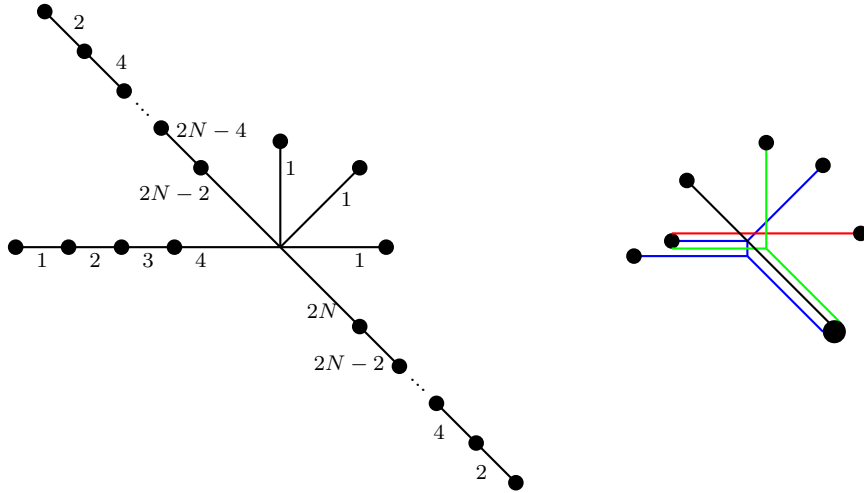**Figure 9**: A unitary web description for the K_N^3 theory, together with the maximal subdivision for the Higgs branch at infinite coupling.

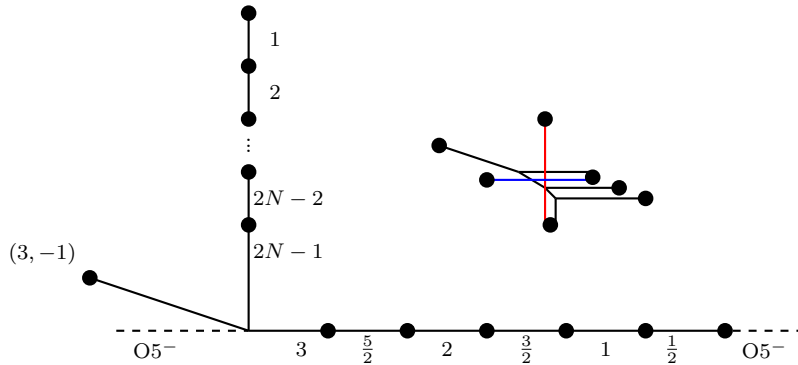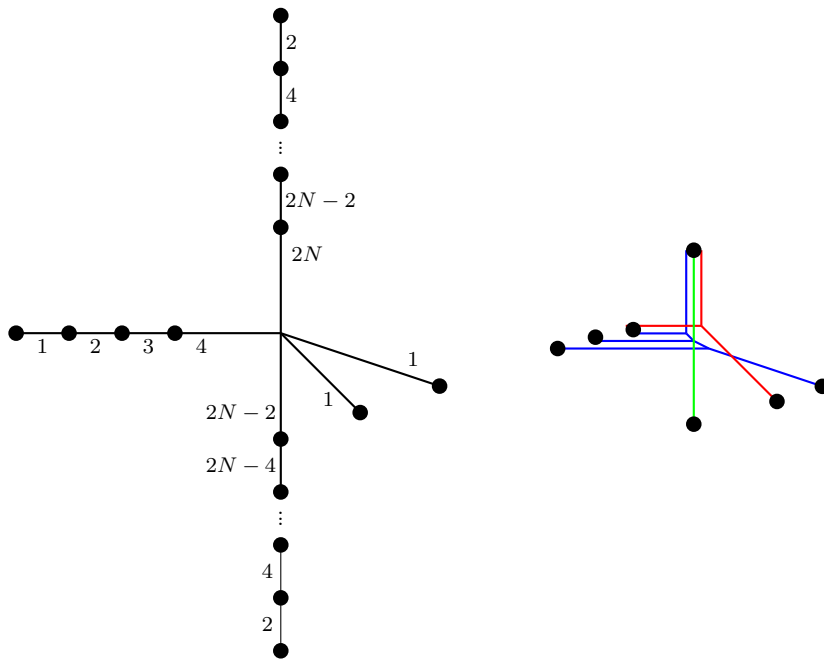**Table 2**: Magnetic quivers for the K_N^p family. The unitary quivers are derived from the unitary web diagrams of figures 5, 7, 9. The orthosymplectic quivers on the other hand come from the orinetifold web diagrams of figures 4, 6 and 8 respectively.

K_N^p	Unitary magnetic quiver $\mathrm{HS}(t)$	Orthosymplectic magnetic quiver	
		$\mathrm{HS}(t; \vec{m} \in \mathbb{Z})$	$\mathrm{HS}(t; \vec{m} \in \mathbb{Z} + \frac{1}{2})$
K_1^1	$1 + 78t + 2430t^2 + 43758t^3 +$ $537966t^4 + 4969107t^5 + \dots$	$1 + 46t + 1278t^2 + 22254t^3 +$ $270798t^4 + 2491731t^5 + \dots$	$32t + 1152t^2 + 21504t^3 +$ $267168t^4 + 2477376t^5 + \dots$
K_2^1	$1 + 30t + 592t^2 + 8867t^3 +$ $106965t^4 + 1073577t^5 + \dots$	$1 + 30t + 496t^2 + 6083t^3 +$ $63477t^4 + 586537t^5 + \dots$	$96t^2 + 2784t^3 + 43488t^4 +$ $487040t^5 + \dots$
K_1^2	$\dfrac{P_3(t)}{(1-t)^{14}}$ $= 1 + 45t + 770t^2 + 7644t^3$ $+52920t^4 + 282744t^5 + \dots$	$\dfrac{P_4(t)}{(1-t)^{14}(1+t)^7}$ $= 1 + 29t + 434t^2 + 4060t^3$ $+27384t^4 + 144312t^5 + \dots$	$\dfrac{P_5(t)}{(1-t)^{14}(1+t)^7}$ $= 16t + 336t^2 + 3584t^3$ $+25536t^4 + 138432t^5 + \dots$
K_2^2	$1 + 25t + 392t^2 + 4590t^3 +$ $42387t^4 + 320549t^5 + \dots$	$1 + 25t + 344t^2 + 3438t^3 +$ $27843t^4 + 191957t^5 + \dots$	$48t^2 + 1152t^3 + 14544t^4 +$ $128592t^5 + \dots$
K_1^3	$\dfrac{1 + 16t + 36t^2 + 16t^3 + t^4}{(1-t)^8}$ $= 1 + 24t + 200t^2 + 1000t^3$ $+3675t^4 + 10976t^5 + \dots$	$\dfrac{P_6(t)}{(1-t)^8(1+t)^4}$ $= 1 + 16t + 120t^2 + 560t^3$ $+1995t^4 + 5824t^5 + \dots$	$\dfrac{P_7(t)}{(1-t)^8(1+t)^4}$ $= 8t + 80t^2 + 440t^3$ $+1680t^4 + 5152t^5 + \dots$
K_2^3	$1 + 24t + 296t^2 + 2510t^3 +$ $16374t^4 + 87306t^5 + \dots$	$1 + 24t + 272t^2 + 2078t^3 +$ $12294t^4 + 60450t^5 + \dots$	$24t^2 + 432t^3 + 4080t^4 +$ $26856t^5 + \dots$

Table 3: Coulomb branch Hilbert series of the unitary and orthosymplectic magnetic quivers for the K_N^p family listed in Table 2. For orthosymplectic quivers, we need to add the contributions of both integer and half integer fluxes. The total Hilbert series then matches with that of the unitary quivers. The explicit forms of $P_3(t), P_4(t), P_5(t), P_6(t), P_7(t)$ are given in Appendix B.

2.3 The $\mathbf{Y}_N$ family

We then consider a different type of decoupling from the $\#_{3,N}$ theory to arrive at different examples which show some new features.

2.3.1 The $\mathbf{Y}_N^{1,1}$ theory

In section 2.2, we decouple flavors of the USp(2) gauge node on one end. Here we decouple one flavor from the USp(2) gauge nodes on the two ends and call the theory $\mathrm{Y}_N^{1,1}$ theory. An IR description of the theory is

$$
\overbrace{[2] - \mathrm{USp}(2) - \mathrm{SO}(6) - \mathrm{USp}(2) - \cdots - \mathrm{SO}(6) - \mathrm{USp}(2)}^{2N+1} - [2] \qquad (2.15)
$$

An orientifold web diagram of the $\mathrm{Y}_N^{1,1}$ theory is obtained by intersecting 2 D5, $2N$ NS5, one $(1,1)$ and one $(1,-1)$ 5-brane on top of an O5-plane, here taken to be asymptotically O5$^-$-plane (Figure 10). The theory also admits a description in terms of an ordinary web which we have shown in Figure 11. The ordinary web description follows either by reading off the low energy gauge theory from an S-dual description or by following a gluing procedure similar to the one described in Figure 2.
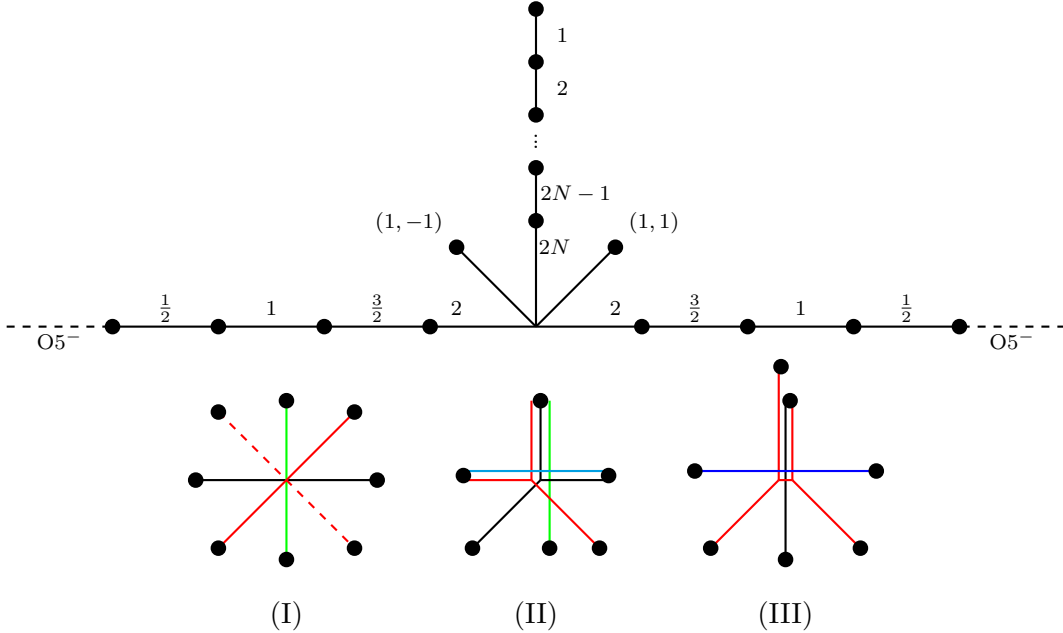

Figure 10: An orientifold web for the $\mathrm{Y}_N^{1,1}$ theory at the fixed point. We show the three possible maximal subdivisions of the centre of the junction at the bottom.

Given the maximal subdivisions in Figure 10 and Figure 11, we can write down the corresponding orthosymplectic and unitary magnetic quivers, the results are collected in
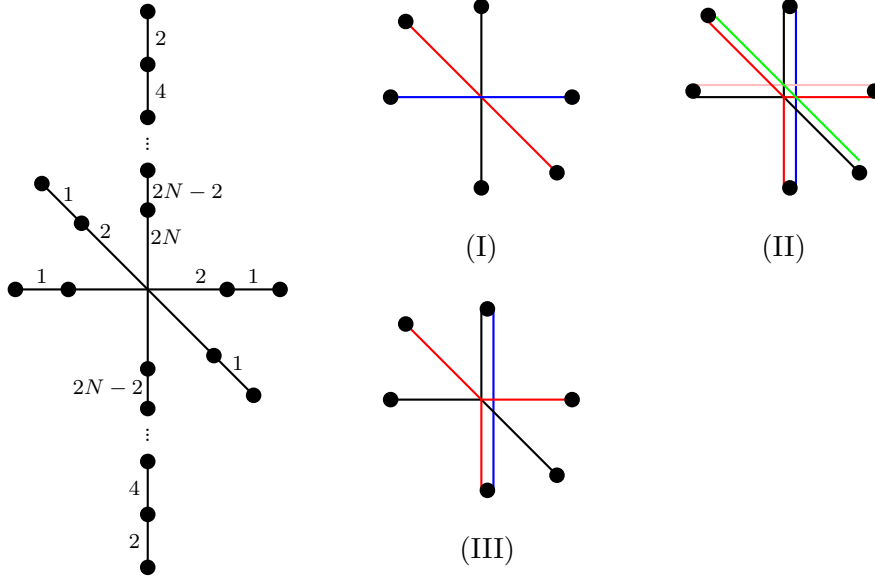
Figure 11: A unitary web for the $Y_N^{1,1}$ theory at the fixed point, along with the three possible distinct maximal subdivisions of the centre of the junction.

Table 4. For the maximal subdivisions labeled as (I) and (III), the magnetic quivers are straightforward to derive. The subdivision (II) requires further clarification. Here we encounter another instance of a new feature appearing in the OSp magnetic quiver. The appearance of an exotic bi-fundamental, denoted by a dashed link in the orthosymplectic quiver in Table 4 corresponding to maximal subdivision (II). To explain the origin, as well as the meaning of this link, we refer to Figure 12. Here we show the subdivisions responsible
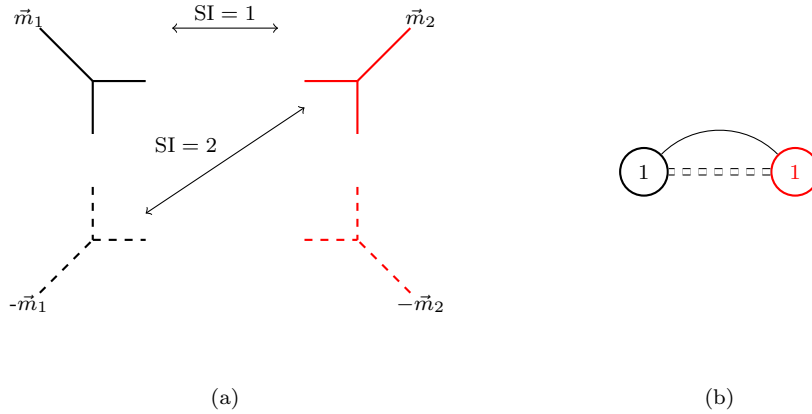
Figure 12: The origin of the exotic bi-fundamental hypermultiplets. (a) The maximal subdivision of the relevant web. The dashed lines correspond to the mirror images of the solid line subwebs. For ease of presentation we have not included the O5-plane in the picture. (b) The corresponding magnetic quiver with the exotic bi-fundamental hypermultiplet.

for the two U(1) nodes from which this link emanates. Denoting the coordinates of the $x^{7,8,9}$

directions, which are the directions where 7-branes extend but 5-branes do not extend, of a given subweb by $\vec{m}_i$, its mirror image must be at coordinate $-\vec{m}_i$. The distance between the upper right and upper left subwebs in, say the x^7 direction, in Figure 12 is therefore given by $|m_1^{(7)} - m_2^{(7)}|$. We claim that this gives rise to an ordinary bi-fundamental hypermultiplet transforming in the $(1, -1)$ representation of $U(1) \times U(1)$. An intuitive explanation of this is that a D3-brane extended between these two subwebs does not feel the presence of the orientifold and is oriented. In contrast, the distance between the upper right subweb and the lower-left subweb (mirror image to upper left) is given by $|m_1^{(7)} + m_2^{(7)}|$. This gives rise to an exotic hypermultiplet transforming as $(1, 1)$ under $U(1) \times U(1)$. Since a D3-brane extending between these two subwebs must cross the orientifold, it is unoriented, which gives an intuitive explanation for the hypermultiplet's democratic nature. The number of each type of hypermultiplet follows, as is standard, by computing the stable intersection number. Altogether, this leads to the magnetic quiver shown in Figure 12. This explains the appearance of the dashed lines in the second row of Table 4. To make the proposal more convincing, we compute the Coulomb branch Hilbert series for the OSp and unitary magnetic quivers. The results are collected in Table 5, and they agree with each other.

Table 4: The unitary and the orthosymplectic magnetic quivers derived from various maximal subdivisions (MS) corresponding to the unitary and the orientifold web diagrams in Figure 11 and Figure 10 respectively for the Higgs branch of $Y_N^{1,1}$ theory.

MS	Unitary magnetic quiver	Orthosymplectic magnetic quiver	
	$\mathrm{HS}(t)$	$\mathrm{HS}(t; \vec{m} \in \mathbb{Z})$	$\mathrm{HS}(t; \vec{m} \in \mathbb{Z} + \frac{1}{2})$
$(\mathrm{I})_{N=1}$	$1 + 16t + 185t^2 + 1585t^3 + 10919t^4 + 62648t^5 + 308937t^6 + 1338676t^7 + 5192925t^8 + 18300090t^9 + 59307538t^{10} + \dots$	$1 + 16t + 153t^2 + 1105t^3 + 6759t^4 + 35992t^5 + 169449t^6 + 713140t^7 + 2714621t^8 + 9447450t^9 + 30359666t^{10} + \dots$	$32t^2 + 480t^3 + 4160t^4 + 26656t^5 + 139488t^6 + 625536t^7 + 2478304t^8 + 8852640t^9 + 28947872t^{10} + \dots$
$(\mathrm{I})_{N=2}$	$1 + 28t + 419t^2 + 4519t^3 + 39592t^4 + 298310t^5 + \dots$	$1 + 28t + 419t^2 + 4423t^3 + 37000t^4 + 261190t^5 + \dots$	$96t^3 + 2592t^4 + 37120t^5 + \dots$
$(\mathrm{II})_{N=1}$	$1 + 18t + 246t^2 + 2266t^3 + 15910t^4 + 89506t^5 + 422730t^6 + 1728642t^7 + 6272807t^8 + 20573244t^9 + 61888524t^{10} + \dots$	$1 + 18t + 198t^2 + 1530t^3 + 9574t^4 + 50466t^5 + 229338t^6 + 914946t^7 + 3266279t^8 + 10596380t^9 + 31638956t^{10} + \dots$	$48t^2 + 736t^3 + 6336t^4 + 39040t^5 + 193392t^6 + 813696t^7 + 3006528t^8 + 9976864t^9 + 30249568t^{10} + \dots$
$(\mathrm{II})_{N=2}$	$1 + 30t + 476t^2 + 5465t^3 + 51395t^4 + 416458t^5 + \dots$	$1 + 30t + 476t^2 + 5305t^3 + 46915t^4 + 350474t^5 + \dots$	$160t^3 + 4480t^4 + 65984t^5 + \dots$
$(\mathrm{III})_{N=1}$	$\dfrac{P_8(t)}{(1-t)^{14}(1+t)^7}$ $= 1 + 13t + 121t^2 + 797t^3 + 4240t^4 + 18760t^5 + \dots$	$\dfrac{P_9(t)}{(1-t)^{14}(1+t+t^2+t^3)^7}$ $= 1 + 13t + 105t^2 + 605t^3 + 2864t^4 + 11640t^5 + \dots$	$\dfrac{P_{10}(t)}{(1-t)^{14}(1+t+t^2+t^3)^7}$ $= 16t^2 + 192t^3 + 1376t^4 + 7120t^5 + \dots$
$(\mathrm{III})_{N=2}$	$1 + 28t + 419t^2 + 4452t^3 + 37756t^4 + 270816t^5 + \dots$	$1 + 28t + 419t^2 + 4388t^3 + 36028t^4 + 246496t^5 + \dots$	$64t^3 + 1728t^4 + 24320t^5 + \dots$

Table 5: Coulomb branch Hilbert series of the unitary and the orthosymplectic magnetic quivers for different maximal subdivisions of the $\mathrm{Y}_N^{1,1}$ theory. The corresponding quivers are presented in Table 4. The explicit forms of $P_8(t), P_9(t), P_{10}(t)$ are given in Appendix B.

2.3.2 The $Y_N^{2\times1,2\times1}$ theory

The examples we consider are brane configurations obtained by intersecting $2N$ NS5, 2 $(1,1)$, 2 $(1,-1)$ and one D5 brane on top of an O5-plane which is asymptotically an O5$^-$-plane. We call the theory on the web the $Y_N^{2\times1,2\times1}$ theory. At low energies the theory is described by the following quiver,

$$
\overbrace{[1S + 1C] - \mathrm{SO}(6) - \mathrm{USp}(2) - \mathrm{SO}(6) - \cdots - \mathrm{USp}(2) - \mathrm{SO}(6)}^{2N+1} - [1S + 1C] \qquad . \tag{2.16}
$$

An orientifold web diagram is given in Figure 19.

It may also be understood as gluing $N-1$ copies of SO(6) with 2 vectors and 2 copies of SO(6) with one vector, one spinor, and one conjugate spinor, by successive gauging of USp(2) subgroups of the global symmetry. This latter viewpoint allows us to construct a unitary web for the same theory, by gluing $N-1$ copies of $\mathrm{SU}(4)_0$ with two second rank antisymmetric hypermultiplets, and 2 copies of $\mathrm{SU}(4)_0$ with 2 fundamentals and one 2nd rank antisymmetric hypermultiplet, via gauging common SU(2) subgroups of the global symmetry. The construction is illustrated in Figure 13. Using this method, we obtain a

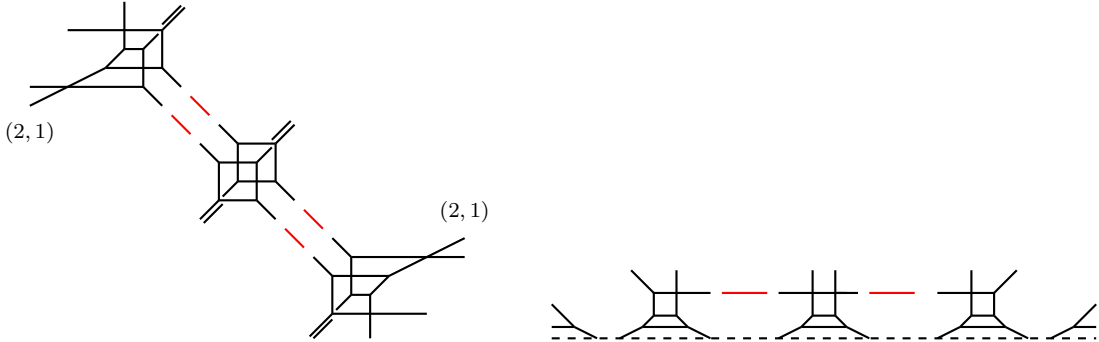**Figure 13**: Constructing web diagrams for $Y_N^{2\times1,2\times1}$ theory by gauging SU(2)'s.

unitary web diagram for the theory of (2.16), and it is depicted in Figure 20.

At infinite coupling, there are 10 maximal subdivisions of the unitary web, of which we only show 8 explicitly in Figure 20. Two further subdivisions are obtained, by 180-degree rotation of those labeled (V) and (VIII) in Figure 20. The unitary magnetic quivers follow straightforwardly and are listed in the second column of Table 6. In the following, we provide a guide to extract the magnetic quivers from the orientifold web.

Consider the maximal subdivision (I) corresponding to the orientifold web in Figure 19. The corresponding orthosymplectic magnetic quiver appears in Table 6. It is a fairly tame object, except for the appearance of the 2 antisymmetric hypermultiplets attached to one of the U(2) nodes. Figure 14 shows the subweb responsible for the U(2) gauge node. There are two $(1,1)$ 5-branes, whose position in the transverse $x^{7,8,9}$ directions are denoted by $\vec{m}_1$ and $\vec{m}_2$ respectively. Consider a D3-brane which is suspended between the $(1,1)$ 5-brane at position $m_1^{(7)}$, and the mirror of the $(1,1)$ 5-brane at position $m_2^{(7)}$, which is
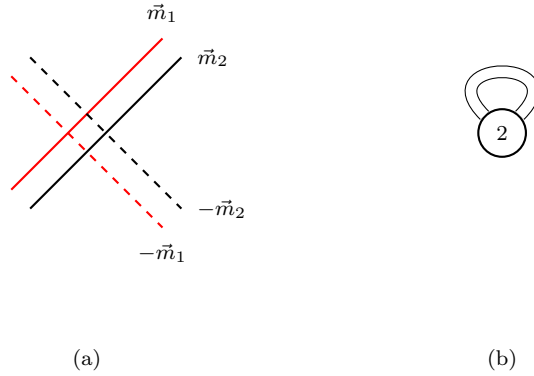
(a)   (b)

Figure 14: The origin of the antisymmetric matter appearing in some magnetic quivers.

located at position $-m_2^{(7)}$ along the x^7 direction. Clearly, the distance between the two subwebs is $|m_1^{(7)}+m_2^{(7)}|$, which is the weight corresponding to the second rank antisymmetric representation of U(2).[5] The fact that there are two such multiplets follows, as is standard, from the stable intersection of the $(1,1)$ and $(1,-1)$ 5-branes. One can repeat this exercise in the presence of n $(1,1)$ 5-branes and their mirror images, and identify the weight system for the second rank antisymmetric representation of U(n) in a similar manner. To make this proposal more concrete, we computed the Coulomb and Higgs branch Hilbert series of the full orthosymplectic magnetic quiver corresponding to maximal subdivision (I) in Table 6. The results are in agreement with the unitary magnetic quiver (see Table 7 for the matching of the Coulomb branch Hilbert series).

Next, consider the maximal subdivision (III) of the orientifold web. Here, we encounter the first example of orientifold web diagrams with identical shapes, that are actually inequivalent. In order to clarify this situation, we start from a much simpler example, known as the rank 1 E_1 SCFT and $\tilde{E}_1$ SCFT [4]. They correspond to the 5d $\mathcal{N} = 1$ pure SU(2) gauge theories with discrete theta angle 0 and π, respectively. When we describe them in terms of the ordinary 5-brane web diagram, there are clear differences, as depicted in Figure 15 [31]. This difference is interpreted as two inequivalent ways of decomposing an
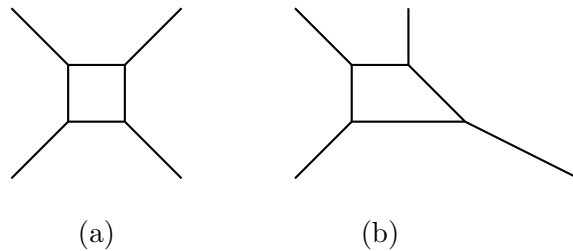

(a)   (b)

Figure 15: Usual 5-brane web diagram for (a) E_1 SCFT and (b) $\tilde{E}_1$ SCFT .

---

[5]In this specific case, the antisymmetric representation of U(2) is a singlet under the SU(2) factor and carries charge 2 under the U(1) factor of the gauge group. However, this should be distinguished from the rule on charge 2 hypermultiplets. For higher rank groups we expect a hypermultiplet transforming under the antisymmetric of U(N).

$O7^-$-plane into two (p, q) 7-branes [53].

The situation in the 5-brane web diagram with O5-plane for these two theories is much subtler. These two web diagrams cannot be distinguished in the weakly coupled phase. However, there are clear difference in another phase as depicted in Figure 16a and 16b [22]. This phase is the counterpart of the phase denoted in [31] as "past infinite coupling". These claims are justified from the analysis of the decompactification limit of the Seiberg-Witten curve obtained from the M5-brane configuration corresponding to these 5-brane webs with O5-plane.
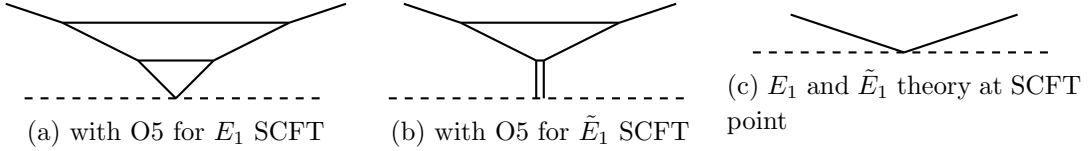

(a) with O5 for E_1 SCFT   (b) with O5 for $\tilde{E}_1$ SCFT   (c) E_1 and $\tilde{E}_1$ theory at SCFT point

Figure 16: 5-brane web diagrams with O5-plane for E_1 and $\tilde{E}_1$ SCFTs.

Suppose that we start from these two different webs and go to SCFT point. Then, the difference disappears at the level of the 5-brane web diagram, as depicted in Figure 16c. However, they should still be distinguished, taking into account that they correspond to two inequivalent 5d SCFT. That is, we should distinguish the 5-brane web diagram in Figure 16c as a limit of Figure 16a, from the 5-brane web diagram in Figure 16c as a limit of Figure 16b. Since we have already known that the former should give non-trivial Higgs branch while the latter should not give any continuous Higgs branch [40], we denote these two webs as "decomposable" web and "not decomposable" web, respectively. This discussion can be generalized to the web diagram where a $(p, 1)$-5 brane and its mirror image are intersecting on top of the $O5^-$-plane for any p. This may be either decomposable to give non-trivial Higgs branch, or not decomposable to give no continuous Higgs branch.

As discussed in [1], we can see only one Higgs branch of the rank 1 E_3 SCFT from naive analysis with the 5-brane web with O5-plane. However, once we accept the claims above, we can reproduce the two different branches of rank 1 E_3 SCFT. Depending on whether the $(2, 1)$ 5-brane in Figure 17 is either decomposable or not decomposable, they lead to two different magnetic quivers:

    (2.17)

Here, not decomposable web, which cannot be detached from the O5-plane, contribute as a flavor. A different example of treating a subweb which cannot be detached from the O5-plane as a flavor is discussed in [1].
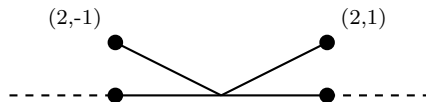

Figure 17: 5-brane web diagram with O5-plane for E_3 SCFT.

Analogous discussion is possible for still another type of 5-brane web. We should distinguish the diagram in Figure 18a as a limit of the diagram in Figure 18b, which is decomposable, and the diagram in Figure 18a as a limit of the diagram in Figure 18c, which is not decomposable. The former can be decomposed in a natural way to give $U(1) \times U(2) \times U(1)$ gauge group in the magnetic quiver while the latter cannot be detached from the O5-plane and thus should be treated as a flavor. This claim is justified by comparing them with the equivalent ordinary 5-brane web diagrams.
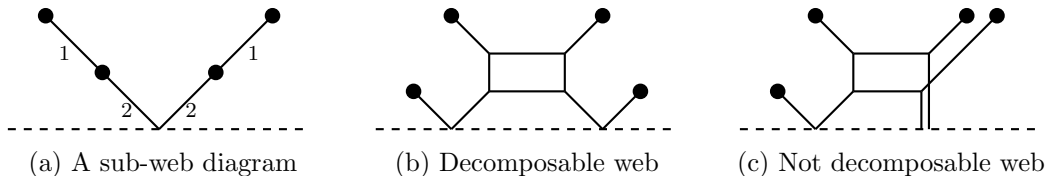

(a) A sub-web diagram   (b) Decomposable web   (c) Not decomposable web

Figure 18: Decomposable and not decomposable orientifold web diagrams in $Y_N^{2\times 1, 2\times 1}$.

Now we go back to the $Y_N^{2\times 1, 2\times 1}$ theory. The orientifold web in Figure 19 includes the subweb in Figure 18a. The maximal subdivision (I) includes the decomposable web, and the maximal subdivision (III) includes a subweb that is not decomposable.

Among the eight maximal subdivisions, the maximal subdivision (V) in Figure 19 yields a magnetic quiver with a charge 2 hypermultiplet. The maximal subdivision (V) contains the subweb in red in the maximal subdivision in Figure 19. We compute the number of the charge 2 hypermultiplets associated with the U(1) gauge node from the subweb by the rule in (2.6). The stable intersection number of the subweb with its mirror is

$$\text{SI of subweb with its own mirror image} = 10 - 2 = 8, \tag{2.18}$$

and the stable intersection number of the subweb with O5 is

$$\text{SI of subweb with O5} = 3. \tag{2.19}$$

Then the number of the charge 2 hypermultiplets from (2.6) is

$$\frac{8}{2} - 3 = 1, \tag{2.20}$$

for the U(1) node associated with the subweb in red of the maximal subdivision (V) in Figure 19.

With the rules described above, we propose the magnetic quivers from the orientifold web for the eight maximal subdivisions and the result is summarized in Table 6. We have checked the matching of the Coulomb branch Hilbert series of the unitary and orthosymplectic magnetic quivers which can be seen from Table 7.

There are a few more possible configurations in the $Y_N^{p,q}$ family. They do not give rise to any new rules, in addition to those already mentioned so far. They do however serve as working examples that demonstrate the validity of the rules proposed above. We refer the curious reader to Appendix D.

Figure 19: An orientifold web for the $Y_N^{2\times1,2\times1}$ theory along with the possible maximal subdivisions at the centre of the junction. The number 2 in figure (VII) indicates that all the red lines correspond to two 5-branes.
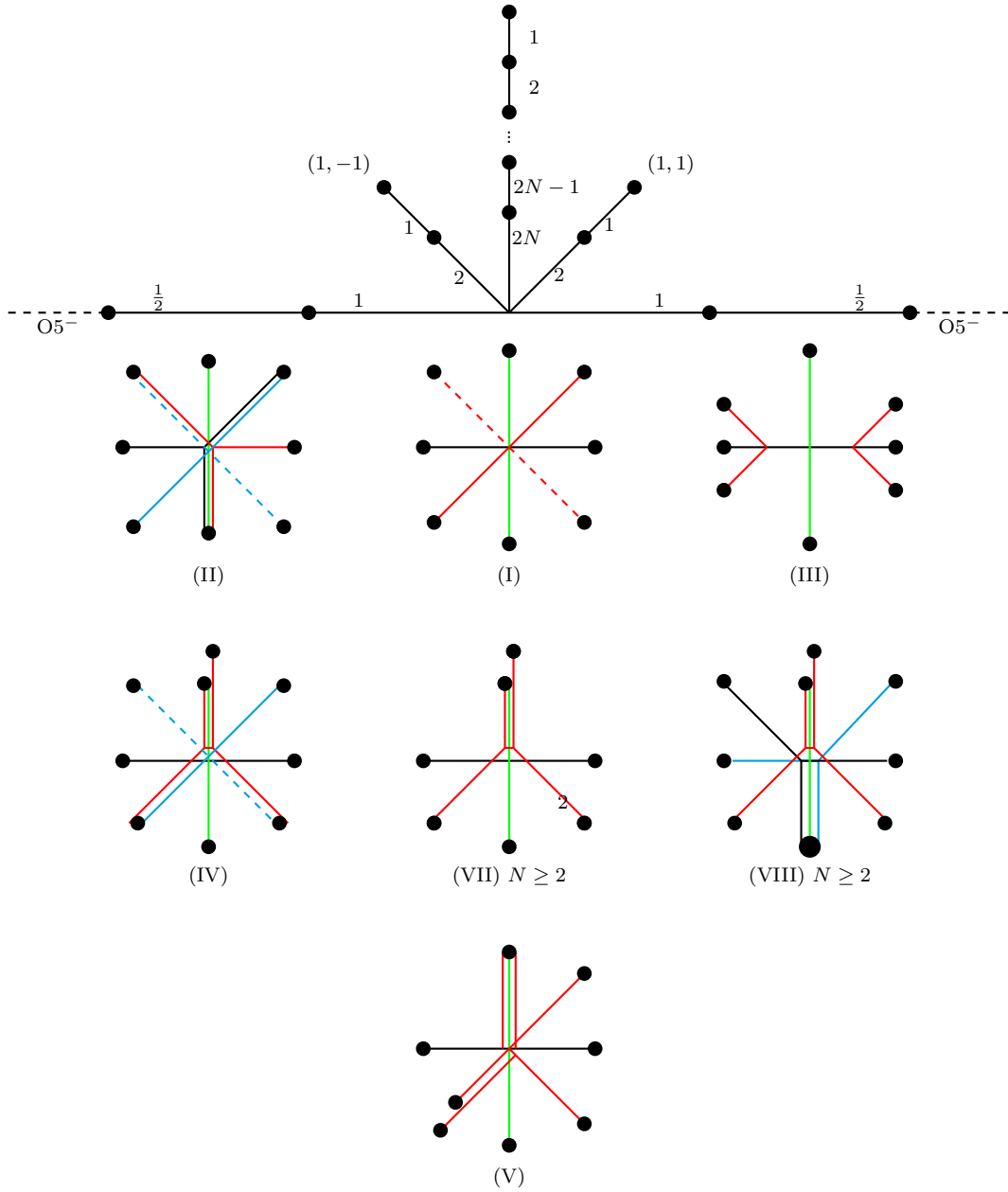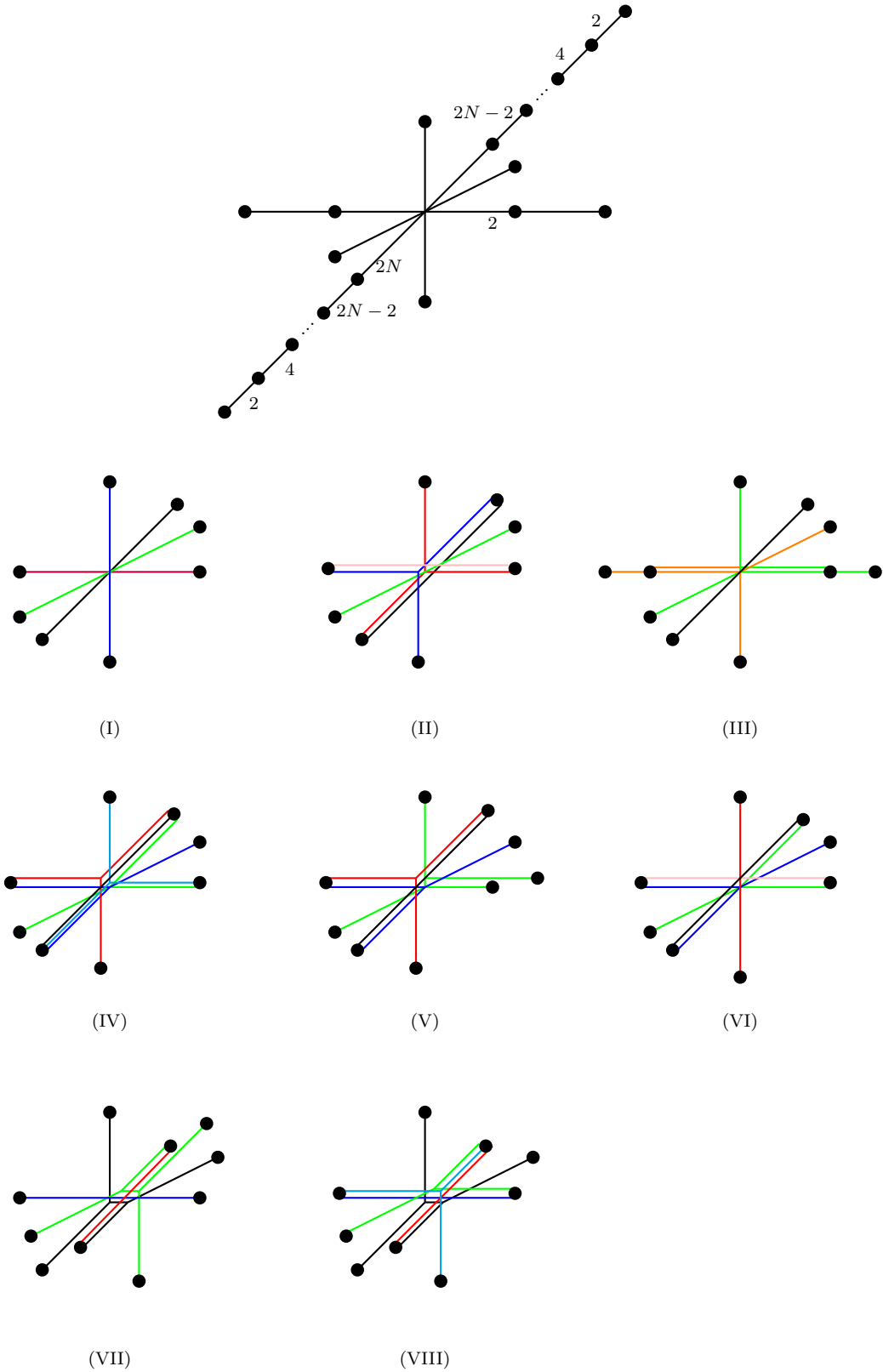
Figure 20: A unitary web diagram for the $Y_N^{2\times1,2\times1}$ theory along with the possible maximal subdivisions at the centre of the junction.

Table 6: Magnetic quivers for various maximal subdivisions (MS) of $Y_N^{2\times 1, 2\times 1}$ theory.

MS	Unitary HS(t)	Orthosymplectic HS$(t; \vec{m} \in \mathbb{Z})$	Orthosymplectic HS$(t; \vec{m} \in \mathbb{Z} + \frac{1}{2})$
$(\mathrm{I})_{N=0}$	$\dfrac{P_{11}(t)}{(1-t)^{10}(1+t)^5}$ $= 1 + 16t + 132t^2 + 735t^3$ $+ 3134t^4 + 10974t^5 + \dots$	$\dfrac{P_{12}(t)}{(1-t)^{10}(1+t)^5(1+t^2)}$ $= 1 + 8t + 72t^2 + 371t^3$ $+ 1598t^4 + 5510t^5 + \dots$	$\dfrac{P_{13}(t)}{(1-t)^{10}(1+t)^5(1+t^2)}$ $= 8t + 60t^2 + 364t^3$ $+ 1536t^4 + 5464t^5 + \dots$
$(\mathrm{I})_{N=1}$	$1 + 11t + 84t^2 + 485t^3 +$ $2346t^4 + 9738t^5 + \cdots$	$1 + 11t + 68t^2 + 317t^3 +$ $1346t^4 + 5290t^5 + \cdots$	$16t^2 + 168t^3 + 1000t^4 +$ $4448t^5 + \cdots$
$(\mathrm{I})_{N=2}$	$1 + 23t + 290t^2 + 2653t^3 +$ $19602t^4 + 123630t^5 + \dots$	$1 + 23t + 290t^2 + 2605t^3 +$ $18522t^4 + 110470t^5 + \dots$	$48t^3 + 1080t^4 + 13160t^5 + \dots$
$(\mathrm{II})_{N=1}$ & $(\mathrm{VI})_{N=1}$	$1 + 12t + 91t^2 + 8t^{5/2} +$ $484t^3 + 104t^{7/2} + 2032t^4 +$ $720t^{9/2} + 7152t^5 + \cdots$	$1 + 12t + 75t^2 + 336t^3 +$ $16t^{7/2} + 1268t^4 + 208t^{9/2} +$ $4220t^5 + \cdots$	$16t^2 + 8t^{5/2} + 148t^3 + 88t^{7/2} +$ $764t^4 + 512t^{9/2} + 2932t^5 + \cdots$
$(\mathrm{II})_{N=2}$ & $(\mathrm{VI})_{N=2}$	$1 + 24t + 313t^2 + 2943t^3 +$ $32t^{7/2} + 22157t^4 +$ $768t^{9/2} + 140921t^5 + \cdots$	$1 + 24t + 313t^2 + 2895t^3 +$ $21089t^4 + 32t^{9/2} +$ $128073t^5 + \cdots$	$48t^3 + 32t^{7/2} + 1068t^4 +$ $736t^{9/2} + 12848t^5 + \cdots$
$(\mathrm{III})_{N=1}$	$\dfrac{P_{14}(t)}{(1-t)^2(1-t^3)(1-t^4)^3}$ $= 1 + 4t + 13t^2 + 33t^3$ $+ 80t^4 + 165t^5 + \cdots$	$\dfrac{P_{14}(t)}{(1-t)^2(1-t^3)(1-t^4)^3}$ $= 1 + 4t + 13t^2 + 33t^3$ $+ 80t^4 + 165t^5 + \cdots$	not required
$(\mathrm{III})_{N=2}$	$1 + 16t + 151t^2 + 1039t^3 +$ $5750t^4 + 26954t^5 + \cdots$	$1 + 16t + 151t^2 + 1039t^3 +$ $5750t^4 + 26954t^5 + \cdots$	not required
$(\mathrm{IV})_{N=1}$	$1 + 9t + 43t^2 + 16t^{5/2} +$ $157t^3 + 128t^{7/2} + 488t^4 +$ $560t^{9/2} + 1400t^5 + \cdots$	$1 + 9t + 43t^2 + 157t^3 +$ $488t^4 + 1400t^5 + \cdots$	$16t^{5/2} + 128t^{7/2} +$ $560t^{9/2} + \cdots$
$(\mathrm{IV})_{N=2}$	$1 + 24t + 313t^2 + 2860t^3 +$ $64t^{7/2} + 20297t^4 +$ $1472t^{9/2} + 118722t^5 + \cdots$	$1 + 24t + 313t^2 + 2860t^3 +$ $20297t^4 + 118722t^5 + \cdots$	$64t^{7/2} + 1472t^{9/2} + \cdots$
$(\mathrm{V})_{N=1}$	$\dfrac{P_{15}(t)}{(1-t)^8(1-t^3)(1-t^5)^3}$ $= 1 + 8t + 34t^2 + 8t^{5/2}$ $+ 106t^3 + 56t^{7/2} + 275t^4$ $+ 216t^{9/2} + 646t^5 + \cdots$	$\dfrac{P_{16}(t)}{(1-t)^8(1-t^3)(1-t^{10})^3}$ $= 1 + 8t + 34t^2 + 106t^3$ $+ 275t^4 + 646t^5 + \cdots$	$\dfrac{8t^{5/2}P_{17}(t)}{(1-t)^8(1-t^3)(1-t^{10})^3}$ $= 8t^{5/2} + 56t^{7/2}$ $+ 216t^{9/2} + \cdots$
$(\mathrm{V})_{N=2}$	$1 + 20t + 224t^2 + 1803t^3 +$ $32t^{7/2} + 11510t^4 +$ $608t^{9/2} + 61468t^5 + \cdots$	$1 + 20t + 224t^2 + 1803t^3 +$ $11510t^4 + 61468t^5 + \cdots$	$32t^{7/2} + 608t^{9/2} + \cdots$
$(\mathrm{VII})_{N=2}$	$1 + 23t + 259t^2 + 1992t^3 +$ $11927t^4 + 59343t^5 + \cdots$	$1 + 23t + 259t^2 + 1944t^3 +$ $11075t^4 + 51523t^5 + \cdots$	$48t^3 + 852t^4 + 7820t^5 + \cdots$
$(\mathrm{VII})_{N=3}$	$1 + 43t + 980t^2 + 15615t^3 +$ $194028t^4 + \cdots$	$1 + 43t + 980t^2 + 15615t^3 +$ $193868t^4 + \cdots$	$160t^4 + \cdots$
$(\mathrm{VIII})_{N=2}$	$1 + 24t + 297t^2 + 2560t^3 +$ $32t^{7/2} + 17229t^4 +$ $736t^{9/2} + 95960t^5 + \cdots$	$1 + 24t + 297t^2 + 2512t^3 +$ $16299t^4 + 32t^{9/2} +$ $86552t^5 + \cdots$	$48t^3 + 32t^{7/2} + 930t^4 +$ $704t^{9/2} + 9408t^5 + \cdots$

Table 7: Coulomb branch Hilbert series of the unitary and orthosymplectic magnetic quivers for different maximal subdivisions (MS) of $Y_N^{2\times 1, 2\times 1}$ theory. The corresponding quivers are presented in Table 6. The explicit forms of $P_{11}(t), \cdots, P_{17}(t)$ are given in Appendix B.

2.4 The H_N family

The final example in section 2 arises from decoupling flavors from the unitary electric quiver for the $\#_{3,N}$ theory (2.3). We denote by $H_N^{p;q}$, the theory obtained by decoupling flavors attached to the central node in (2.3). Here p (q) are the number of flavors integrated out with positive (negative) mass such that $M = 2N - p - q$. In other words, the $H_N^{p;q}$ theory is nothing but

$$
\begin{array}{c}
[M] \\
| \\
\text{SU}(N) - \text{SU}(2N)_{\frac{p-q}{2}} - \text{SU}(N)
\end{array}
\qquad . \tag{2.21}
$$

The unitary and orientifold web diagram for the $H_N^{p;q}$ theory is obtained from those of $+_{3,N}$ theory, i.e. Figure 3 and Figure 1 respectively. Note that in the orientifold web of Figure 1, the desirable mass deformation corresponds to the position of the external NS5 branes along the horizontal axis, a fact which is more transparent in the S-dual frame. Thus the orientifold web description of the $H_N^{p;q}$ theory is obtained from that of $+_{3,N}$ theory by decoupling, say, p of the external NS5 branes to the left, and q to the right.

Let us focus on the case with $p = q = N$. The 5d theory (2.21) becomes

$$
\text{SU}(N) - \text{SU}(2N)_0 - \text{SU}(N). \tag{2.22}
$$

When $N = 1$, the 5d theory is simply the SU(2) gauge theory with four flavors. The orientifold web diagram and the unitary web diagram at the infinitely strong coupling of the theory (2.22) are depicted in Figure 21 and Figure 22 respectively. An interesting point
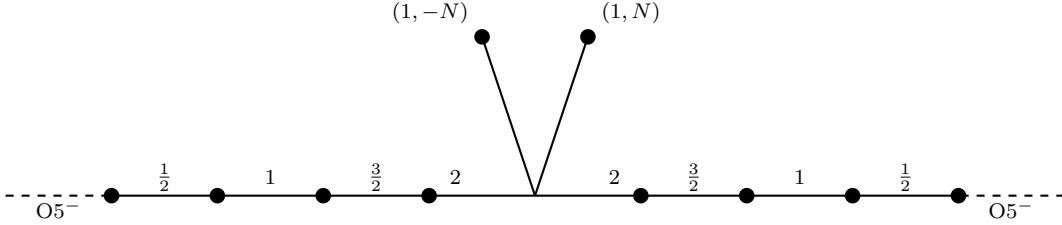

Figure 21: The orientifold web diagram for the $H_N^{N,N}$ theory at the infinitely strong coupling.

about the orientifold web diagram in Figure 21 is that the diagram has $(1, N)$ and $(1, -N)$ 5-branes where N can be larger than 1 and they intersect on the orientifold plane. This is a new feature which has not appeared in the past web diagrams. Hence this example is important for checking the rule (2.6) for the number of charge 2 hypermultiplets attached to the U(1) gauge node originated from the $(1, N)$ and $(1, -N)$ 5-branes with $N \geq 2$[6]. From the web diagrams it is possible to infer the corresponding magnetic quiver theories and we argue that they are the ones given in Table 8. Note that the number of the charge 2 hypermultiplets attached to the $U(1)$ gauge node in the orthosymplectic magnetic quiver is

---

[6]We will consider cases which involve (p, q) and $(p, -q)$ 5-branes with both p and q larger than 1 in Appendix C.

$$\left(\frac{N_{\text{even}}}{2}, -1\right) \text{ or } \left(\frac{N_{\text{odd}}-1}{2}, -1\right) \qquad \left(\frac{N_{\text{even}}}{2}, 1\right) \text{ or } \left(\frac{N_{\text{odd}}+1}{2}, 1\right)$$
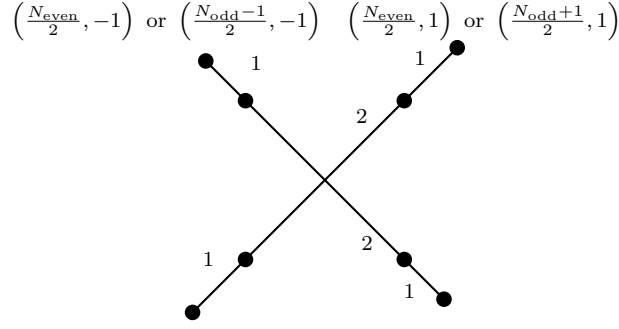
Figure 22: The unitary web diagram for the $H_N^{N,N}$ theory at the infinitely strong coupling.

$H_N^{p,q}$	Unitary magnetic	Orthosymplectic magnetic
$H_N^{N,N}$		

Table 8: Magnetic quivers for the $H_N^{N,N}$ family. The index N in each figure denotes the number of the hypermultiplets.

$H_N^{N,N}$	Unitary magnetic quiver	Orthosymplectic magnetic quiver	
	$\text{HS}(t)$	$\text{HS}(t; \vec{m} \in \mathbb{Z})$	$\text{HS}(t; \vec{m} \in \mathbb{Z} + \frac{1}{2})$
$H_2^{2,2}$	$1 + 13t + 121t^2 + 797t^3 +$ $4240t^4 + 18760t^5 + \cdots$	$1 + 13t + 105t^2 + 605t^3 +$ $2864t^4 + 11640t^5 + \cdots$	$16t^2 + 192t^3 + 1376t^4 +$ $7120t^5 + \cdots$
$H_3^{3,3}$	$1 + 13t + 89t^2 + 461t^3 +$ $2007t^4 + 7579t^5 + \cdots$	$1 + 13t + 89t^2 + 445t^3 +$ $1815t^4 + 6347t^5 + \cdots$	$16t^3 + 192t^4 + 1232t^5 + \cdots$
$H_4^{4,4}$	$1 + 13t + 89t^2 + 429t^3 +$ $1671t^4 + 5659t^5 + \cdots$	$1 + 13t + 89t^2 + 429t^3 +$ $1655t^4 + 5467t^5 + \cdots$	$16t^4 + 192t^5 + \cdots$
$H_5^{5,5}$	$1 + 13t + 89t^2 + 429t^3 +$ $1639t^4 + 5323t^5 + \cdots$	$1 + 13t + 89t^2 + 429t^3 +$ $1639t^4 + 5307t^5 + \cdots$	$16t^5 + \cdots$

Table 9: Coulomb branch Hilbert series of the unitary and orthosymplectic magnetic quivers for the $H_N^{N,N}$ family whose quivers are presented in Table 8.

zero due to (2.6). Indeed with this number for the charge 2 hypermultiplets we find perfect agreement between the Coulomb branch Hilbert series of the unitary and orthosymplectic magnetic quiver theories. We summarize the Coulomb branch Hilbert series of the magnetic quivers in Table 8 for various N in Table 9.

3 Magnetic quivers from $O5^+$ - $O5^+$

Next we consider examples which arise from brane configurations with asymptotic $O5^+$-planes on both the ends.

3.1 The $+_{1,N}$ theory

Intersecting $2N$ NS5s, and a single D5 on top of on orientifold plane that is asymptotically an O5$^+$-plane, we arrive at the $+_{1,N}$ theory (Figure 23). It has an IR gauge theory description as

$$
[1] - \overbrace{\mathrm{SO}(6) - \mathrm{USp}(2) - \mathrm{SO}(6) - \cdots - \mathrm{USp}(2) - \mathrm{SO}(6)}^{2N-1} - [1] \qquad . \qquad (3.1)
$$

It can also be understood as gluing N copies of SO(6) with two vector hypermultiplets by successive gauging of USp(2) subgroups of the flavour symmetry. One can therefore engineer the same theory with an ordinary web diagram by gluing together N copies of $\mathrm{SU}(4)_0$ with 2 antisymmetric hypermultiplets, via successive gauging of SU(2) subgroups of the global symmetry (Figure 24).

In this setup, the $2N$ NS5-branes intersecting with the O5$^+$-plane contribute to the magnetic quiver as a USp($2N$) gauge node. Here, we claim that there is a new feature in this case, which did not appear for NS5-branes intersecting with O5$^-$-plane. In order for the orthosymplectic magnetic quiver to give consistent results with the corresponding unitary quiver, we find that we need to add three fundamental half-hypermultiplets on this USp($2N$) gauge node.

We would like to interpret these three half-hypermultiplets as follows. First, we observe that the RR charge of the O5$^+$-plane is identical to the sum of the RR charges of O5$^-$-plane and of four half D5-branes. This motivates us to treat O5$^+$-plane as if it is the composite of them:

$$
(\text{O5}^+\text{-plane}) = (\text{O5}^-\text{-plane}) + 4 \times (\text{Half D5 branes}). \qquad (3.2)
$$

Here, we assume that the half D5 branes cannot be detached from the O5$^-$-plane. Basically, the charge 1 hypermultiplet can be reinterpreted as coming from the D3-branes suspended between the NS5-branes and these half D5-branes. However, we need a further explanation of why the number of half-hypermultiplets is three instead of four. In this setup, there are two half D5-branes on top of the O5$^+$-plane, producing SO(3) gauge group in the magnetic quiver. We would like to interpret that one out of the four half D5-branes inside the O5$^+$-plane is used for constructing an SO(3) gauge group. In other words, the D3-brane suspended between the NS5-branes and this half D5-brane contributes as a part of the bi-fundamental hypermultiplets between the USp($2N$) node and the SO(3) node. This indicates that only the remaining three out of the four half D5-branes contribute as fundamental half-hypermultiplets.

Under this assumption, we find the agreement between the Hilbert series of the orthosymplectic quiver in Figure 25b and the Hilbert series of the unitary quiver in Figure 25a both for the Coulomb branches and for the Higgs branches. In particular, the Higgs branch Hilbert series matching is crucial to settle the question about whether the O(1) $\simeq \mathbb{Z}_2$ nodes in the orthosymplectic quiver are flavor or gauge nodes. Such a match is only obtained if

$\mathbb{Z}_2$ gaugings are assumed. The obtained result is:

$$\text{HS}_H(t^2) = 1 + 3t^2 + 15t^4 + 36t^6 + 98t^8 + \cdots . \tag{3.3}$$

The results of the Coulomb branch Hilbert series is tabulated in Table 10.

Encouraged by this agreement, we propose the following rule for the USp($2N$) gauge node coming from the $2N$ NS5-branes intersecting with O5$^+$-plane. If this USp($2N$) gauge node has a bi-fundamental hypermultiplet with the SO(odd) gauge node coming from the D5-branes on the O5$^+$-plane, there are three fundamental half-hypermultiplets. Otherwise, there are four fundamental half-hypermultiplets.
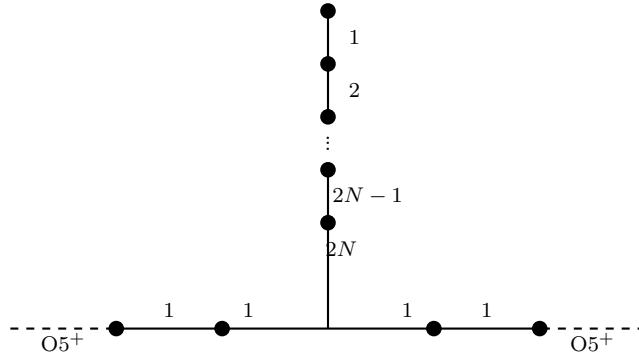
Figure 23: An orientifold web of the $+_{1,N}$ theory with asymptotically O5$^+$ orientifold planes at strong coupling.
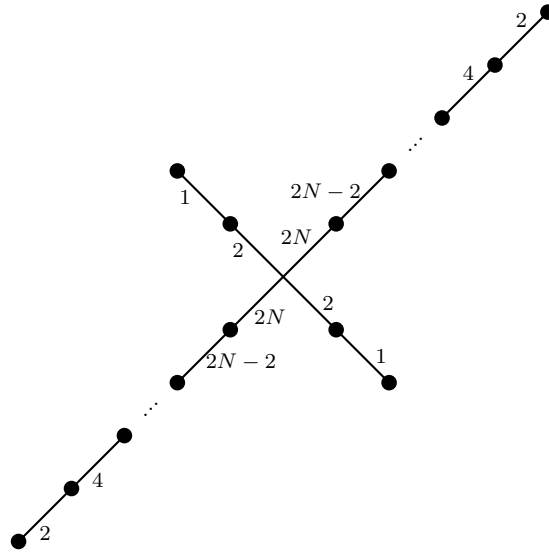

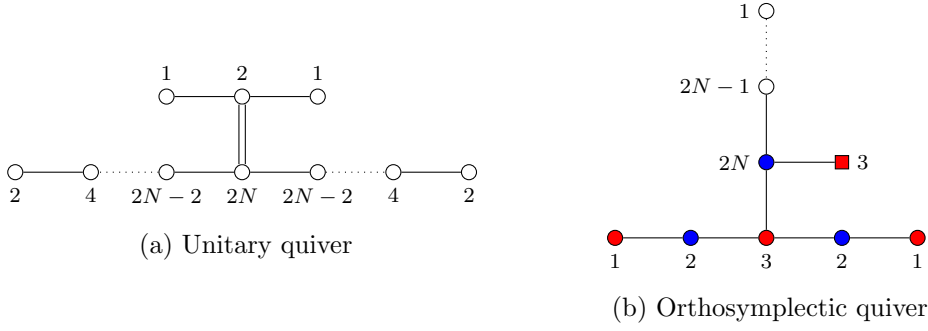**Figure 24**: A unitary web for the $+_{1,N}$ theory with asymptotically O5$^+$ orientifold planes.

(a) Unitary quiver

(b) Orthosymplectic quiver

Figure 25: Magnetic quivers for the $+_{1,N}$ theory

$+_{1,N}$	Unitary magnetic quiver	Orthosymplectic magnetic quiver	
	$\text{HS}(t)$	$\text{HS}(t; \vec{m} \in \mathbb{Z})$	$\text{HS}(t; \vec{m} \in \mathbb{Z}+\frac{1}{2})$
$+_{1,1}$	$\dfrac{P_{18}(t)}{(1-t)^{10}\,(1+t)^5}$ $= 1 + 13t + 100t^2 + 527t^3$ $+2174t^4 + 7425t^5 + \cdots$	$\dfrac{P_{18}(t)}{(1-t)^{10}\,(1+t)^5}$ $= 1 + 13t + 100t^2 + 527t^3$ $+2174t^4 + 7425t^5 + \cdots$	not required
$+_{1,2}$	$1 + 21t + 249t^2 + 2188t^3 +$ $15657t^4 + 95340t^5 + \cdots$	$1 + 21t + 249t^2 + 2188t^3 +$ $15657t^4 + 95340t^5 + \cdots$	not required

Table 10: Coulomb branch Hilbert series for the unitary and orthosymplectic magnetic quivers in Figure 25a and Figure 25b for the $+_{1,N}$ theory. The explicit form of $P_{18}(t)$ is given in Appendix B.

3.2   The $\hat{K}_N^1$ theory

Decoupling a single flavor from, say, the leftmost node in the $+_{1,N}$ theory (3.1), one arrives at the $\hat{K}_N^1$ theory. It has an IR gauge theory description as

$$\overbrace{\text{SO}(6) - \text{USp}(2) - \text{SO}(6) - \cdots - \text{USp}(2) - \text{SO}(6)}^{2N-1} - [1] \tag{3.4}$$

We depict the orientifold and unitary web in Figure 26 and Figure 27 respectively.

Also, in this setup, we find $\text{USp}(2N-2)$ gauge node coming from the $2N-2$ NS5-branes intersecting with the O5^+-plane. According to the proposal in the previous subsection, there are four fundamental half hypermultiplets for this node because there is no SO(odd) gauge node coupled to this $\text{USp}(2N-2)$ gauge node.

In addition, there is one subweb intersecting with the O5^+-plane, contributing as a U(1) gauge node of the magnetic quiver. In general, when a subweb is intersecting with the O5^+-plane, it would be reasonable to expect that there are contributions from the D3-branes suspended between the considered subweb and its mirror image. Analogous to the case with O5^--plane, such contribution is the hypermultiplets with charge 2 coupled to the corresponding U(1) node. The number of such charge 2 hypermultiplets would be
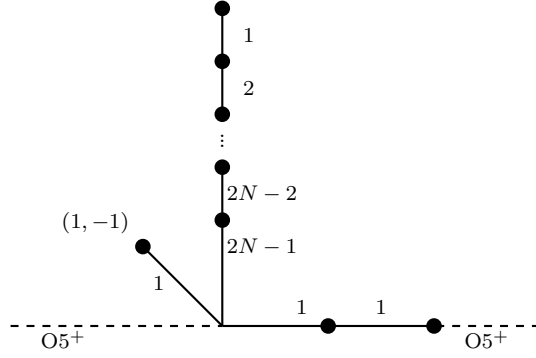
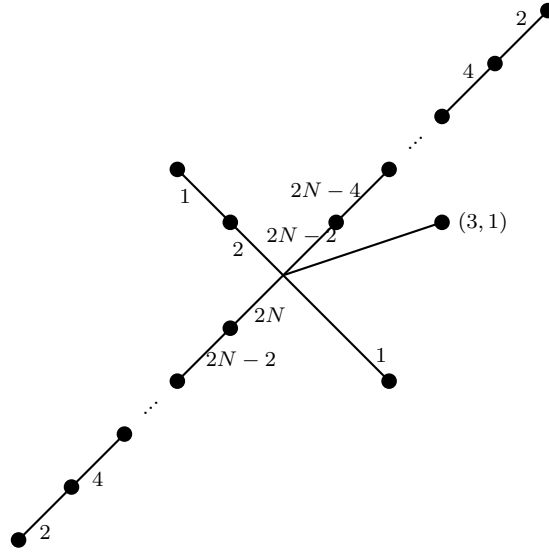**Figure 26**: An orientifold web for the $\hat{K}_N^1$ theory with asymptotically O5$^+$ planes

Figure 27: A unitary web for the $\hat{K}_N^1$ theory with asymptotically O5$^+$ orientifold planes.

given schematically by

$$\frac{\text{(SI with its mirror image)}}{2} - \text{(SI with O5}^+\text{)}, \tag{3.5}$$

as discussed around (2.6). In this specific setup, the number of the charge 2 hypermultiplets should be zero, in order to agree with the unitary magnetic quiver.

However, again, the situation for such U(1) node is different from the case with O5$^-$-plane. Analogous to the case with NS5-branes intersecting with the O5$^+$-plane, the idea discussed around (3.2) implies that there is a contribution from the D3-branes suspended between this subweb and the half D5-branes included in the O5$^+$-plane. Such D3-branes correspond to hypermultiplets with charge 1 instead of charge 2 because the distance between the considered subweb and the O5$^+$-plane is half the distance between the original subweb and its mirror image. In order for the orthosymplectic magnetic quiver to be consistent with the unitary quiver, we need three hypermultiplets with charge 1 coupled

to the U(1) node. This three is interpreted as

$$4(\text{bare SI with half D5}) - (\text{Contribution from the common half D7 on the O5}^+). \quad (3.6)$$

In our case, bare SI with half D5-brane is one. The contribution from the half D7-brane is also one because the considered subweb and the half D5 are both attached to the common half D7-brane from the same direction.[7] We propose that the number of charge 1 hypermultiplets coupled to the U(1) node is given by (3.6) in general. The contribution from the common half D7-brane on the O5$^+$-plane is computed analogously to the case for the unitary quiver discussed in [45].

To support this proposed rule, we match the Higgs branch Hilbert series for the unitary and the orthosymplectic magnetic quiver, especially to settle the question of whether the $\mathbb{Z}_2$ node is gauge or flavor. We find that only choosing the $\mathbb{Z}_2$ node to be gauge we recover the correct match. We computed the Hilbert series for both $N = 2$ and $N = 3$, and the result is tabulated in Table 11.
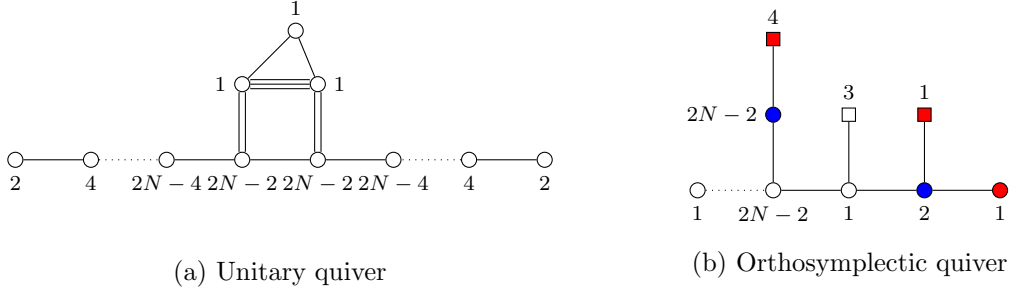

(a) Unitary quiver

(b) Orthosymplectic quiver

Figure 28: Magnetic quivers for the $\hat{K}_N^1$ theory

$\hat{K}_N^1$	Unitary magnetic quiver $\text{HS}_{\mathbb{H}}(t)$	Orthosymplectic magnetic quiver $\text{HS}_{\mathbb{H}}(t)$
$\hat{K}_2^1$	$1 + 9t^2 + 6t^3 + 36t^4 + 36t^5 + 112t^6 + 120t^7 +$ $285t^8 + \dots$	$1 + 9t^2 + 6t^3 + 36t^4 + 36t^5 + 112t^6 + 120t^7 +$ $285t^8 + \dots$
$\hat{K}_3^1$	$1 + 16t^2 + 6t^3 + 150t^4 + 86t^5 + 981t^6 + \dots$	$1 + 16t^2 + 6t^3 + 150t^4 + 86t^5 + 981t^6 + \dots$

Table 11: Higgs branch Hilbert series of the unitary and orthosymplectic magnetic quivers presented in Figure 28.

3.3 The $X_N^{1,1}$ theory

We then consider the configuration obtained by intersecting $2N$ NS5s, one $(1, 1)$, and one $(1, -1)$ on top of an O5$^+$-plane (Figure 29). We call the theory on the web the $X_N^{1,1}$ theory. There is a corresponding IR gauge theory description as

---

[7]When we compute the contribution from the common half D7-brane on the O5$^+$-plane, we treat it as if there were only a single half D5-brane terminated at the common half D7-brane. We do not multiply 4 for this contribution contrary to the contribution from SI.
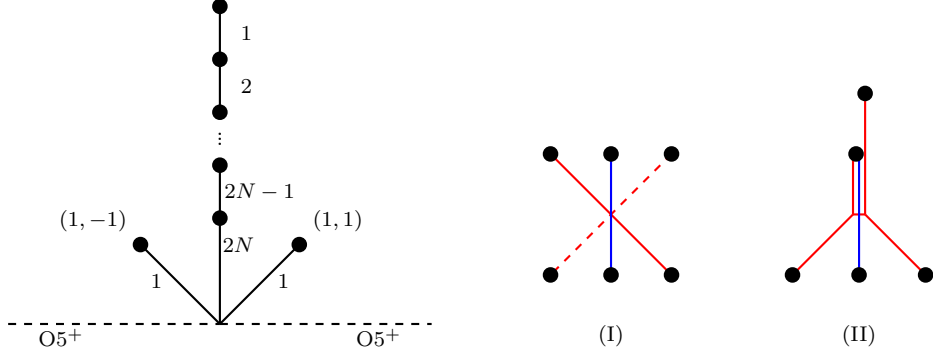
Figure 29: An orientifold web for the $X_N^{1,1}$ theory with asymptotically O5$^+$ planes. We show the two possible maximal subdivisions on the right.

$$\overbrace{\text{SO}(6) - \text{USp}(2) - \text{SO}(6) - \cdots - \text{USp}(2) - \text{SO}(6)}^{2N+1} \tag{3.7}$$

Alternatively, it may be understood as gluing $N-1$ copies of SO(6) with 2 vectors and two copies of SO(6) with one vector, via successive gauging of USp(2) subgroups of the flavour symmetry. This allows us to construct a unitary web for this theory by gluing $N-1$ copies of $\text{SU}(4)_0$ with 2 antisymmetric hypermultiplets and two copies of $\text{SU}(4)_0$ with one antisymmetric hypermultiplet, via successive gauging of SU(2) subgroups of the global symmetry (Figure 30).
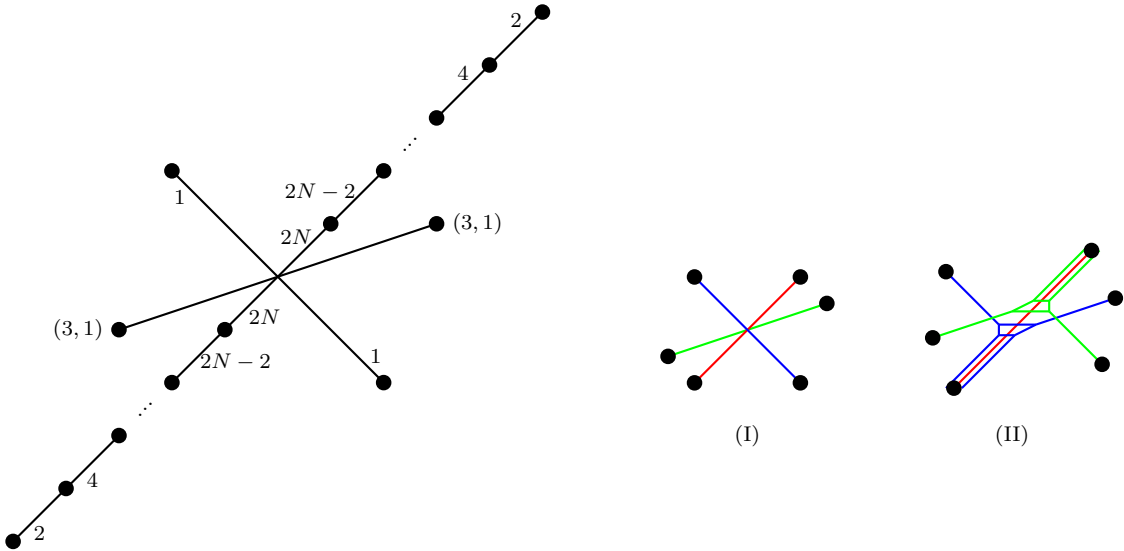

Figure 30: A unitary web for the $X_N^{1,1}$ theory with asymptotically O5$^+$ orientifold planes. The two possible maximal subdivisions are shown on the right.

Table 12: Magnetic quivers corresponding to the maximal subdivisions for the $X_N^{1,1}$ theory.

MS	Unitary magnetic quiver	Orthosymplectic magnetic quiver	
	HS(t)	HS($t; \vec{m} \in \mathbb{Z}$)	HS($t; \vec{m} \in \mathbb{Z} + \frac{1}{2}$)
$(I)_{N=1}$	$\dfrac{P_{19}(t)}{(1-t)^2 (1-t^3) (1-t^4)^3}$ $= 1 + 4t + 13t^2 + 33t^3$ $+ 80t^4 + 165t^5 + \cdots$	$\dfrac{P_{19}(t)}{(1-t)^2 (1-t^3) (1-t^4)^3}$ $= 1 + 4t + 13t^2 + 33t^3$ $+ 80t^4 + 165t^5 + \cdots$	not required
$(I)_{N=2}$	$1 + 16t + 151t^2 + 1039t^3 +$ $5750t^4 + 26954t^5 + \cdots$	$1 + 16t + 151t^2 + 1039t^3 +$ $5750t^4 + 26954t^5 + \cdots$	not required
$(II)_{N=2}$	$1 + 16t + 151t^2 + 1004t^3 +$ $5198t^4 + 22184t^5 + \cdots$	$1 + 16t + 151t^2 + 1004t^3 +$ $5198t^4 + 22184t^5 + \cdots$	not required
$(II)_{N=3}$	$1 + 36t + 701t^2 + 9659t^3 + \cdots$	$1 + 36t + 701t^2 + 9659t^3 + \cdots$	not required

Table 13: Coulomb branch Hilbert series for the unitary and orthosymplectic magnetic quivers presented in Table 12. The explicit form of $P_{19}(t)$ is provided in Appendix B.

The magnetic quivers for the $X_N^{1,1}$ theory are given in Table 12 and the Coulomb branch Hilbert series are tabulated in Table 13.

4 Magnetic quivers from O5$^-$ - O5$^+$

So far we have focused on the configurations where the two asymptotic orientifold planes are of the same type. It is possible to consider cases with an O5$^-$-plane on one end and an O5$^+$-plane on the other end. We will consider such examples in this section.

4.1 The $+_N^{3,1}$ theory

For obtaining the configuration which has an O5$^-$-plane on one end and an O5$^+$-plane on the other end, we decouple one USp(2) part from the quiver in (2.1) for $M = 3$. An IR

quiver description of the theory is

$$\overbrace{[1]\text{-SO}(6) - \text{USp}(2) - \text{SO}(6) - \cdots - \text{USp}(2) - \text{SO}(6)}^{2N-2} - \text{USp}(2) - [3].$$

(4.1)

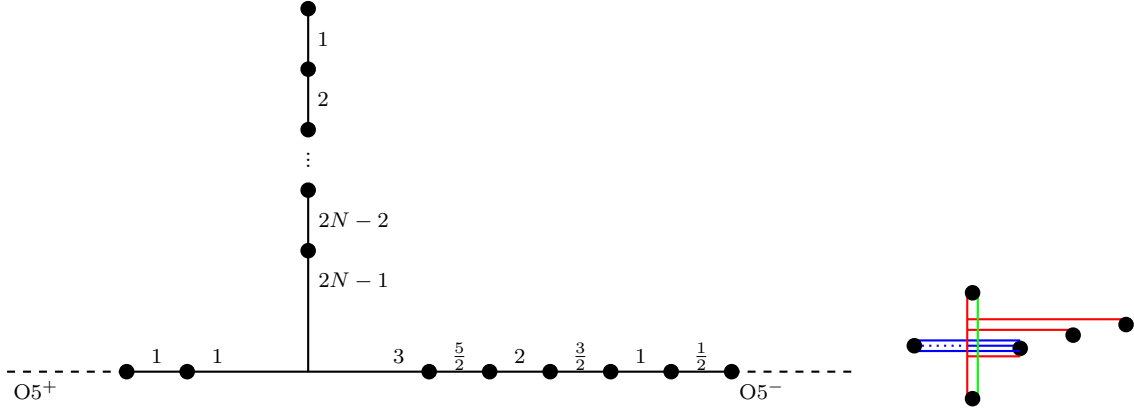The orientifold web for the $+_N^{3,1}$ theory is presented in Figure 31.

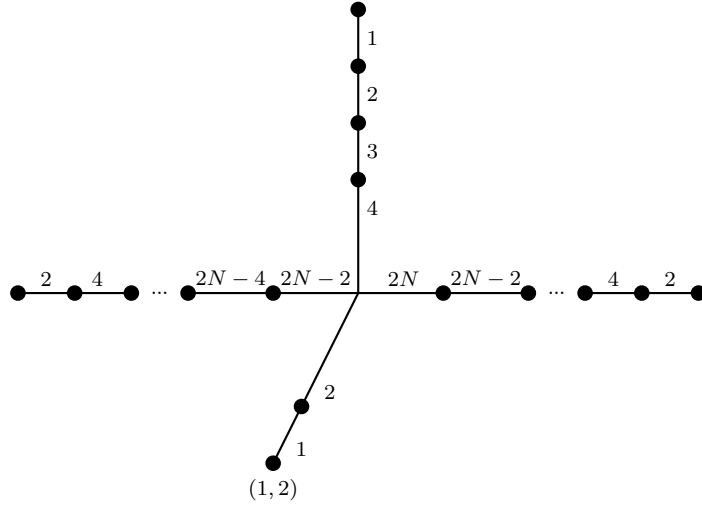**Figure 31**: Orientifold web diagram for the $+_N^{3,1}$ theory.

Figure 32: Unitary web diagram for $+_N^{3,1}$ theory.

The corresponding unitary web is depicted in Figure 32, which is obtained as follows: We first interpret the $+_N^{3,1}$ theory as a decoupling limit from the $\#_{3,N}$ theory. The discussion will be clearer when we discuss this decoupling limit in the S-dual description. The S-dual description of the $\#_{3,N}$ theory has a low energy description as a 5d D_3 quiver gauge theory as given in (2.3). The corresponding 5-brane web for this 5d D_3 quiver gauge theory with $N = 2$ is depicted in Figure 33, which is related to the web diagram in Figure 1 by S-duality as well as "generalized flop transition" discussed in [22]. The decoupling limit is
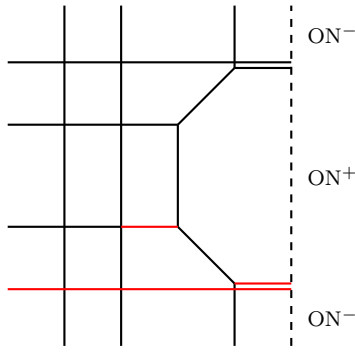
Figure 33: S-dual of $\#_{3,2}$ theory. We move four red D5-branes downward for decoupling.
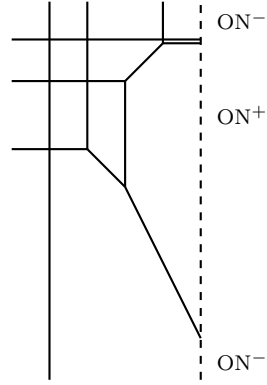

Figure 34: 5-brane web for $+_N^{3,1}$ theory obtained from $\#_{3,2}$ theory by the decoupling limit.
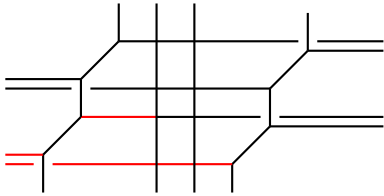

Figure 35: Usual 5-brane web for A_3 quiver for $N = 2$. We move four red D5-branes downward for decoupling.
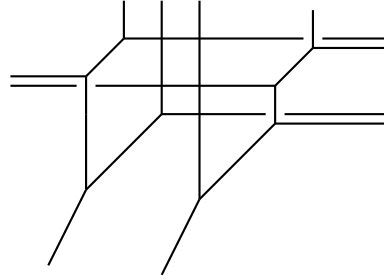

Figure 36: 5-brane web obtained from the A_3 quiver by the decoupling.

to move the red D5-branes downward while keeping the other D5-branes' positions intact, as in Figure 33. These D5-branes are the lowest color branes for each gauge node and the lowest flavor brane charged under the central SU(2N). By this decoupling limit, we obtain the 5-brane web in Figure 34, which is the S-dual description of the $+_N^{3,1}$ theory. Since $D_3 = A_3$, we can consider the corresponding decoupling process also in the ordinary 5-brane web. The ordinary 5-brane web for the A_3 quiver gauge theory is depicted in Figure 35. The corresponding decoupling limit is again to move the red D5-branes downward while keeping the other D5-branes' positions intact, as in Figure 35. Then, we obtain a 5-brane web depicted in Figure 36. Since it is obtained from the same decoupling limit from the $\#_{3,N}$ theory, this should correspond to the $+_N^{3,1}$ theory. The strong coupling limit of Figure 36 gives Figure 32 after S-duality. Although this explanation is for the case with $N = 2$, generalization for generic N is straightforward.

The main part of the maximal subdivision of the orientifold web is given in Figure 31. One of the new features in this example compared to the ones in the previous sections is the dotted blue line on the O5$^+$-plane connected to the ordinary blue line on the O5$^-$-plane. The dotted blue line represents one of the four half D5-branes included in the O5$^+$-plane, which is based on the interpretation discussed around (3.6), while the ordinary blue line is the half D5-brane coming from the three full D5-branes on the O5$^-$-plane. Together with

the other two ordinary blue half D5-branes, it contributes as a SO(3) gauge node in the OSp magnetic quiver in Figure 37. Since three half D5-branes are consumed to construct the SO(3) gauge node, three red half D5-branes remain on the O5$^-$-plane. Due to the charge conservation and the s-rule, the red part, as well as O5-plane, should be treated as one subweb, where the number of half D5 branes reduce by one as we go over half D7-branes to the right. Due to this red subweb, the SO(3) gauge node appears from the part where there are originally two full D5-branes on the O5$^-$-plane because a single half D5-brane is used as a part of the red subweb, and only three half D5-branes remain in this region. This red subweb cannot be detached from the O5-plane because there is no mirror pair and thus contributes as fundamental hypermultiplet to various gauge nodes. The number of half hypermultiplets is obtained by computing the stable intersection number between the subweb corresponding to the considered gauge node and this red subweb, which includes both the original and its mirror image. For example, the stable intersection number between the red subweb and the green NS5-brane is three. However, they both attach to the same (0,1) 7-branes from the same direction at the two places, including the mirror image so that the number of the half-hypermultiplets for the USp($2N - 2$) gauge node is $3 - 2 = 1$. Or, equivalently, we could have considered that the green NS5-branes are placed to the left of the red subweb so that it does not intersect with it. In this case, we should regard that the green NS5-branes are intersecting with O5$^+$-plane. Then, the rule discussed below (3.6) enables us to reinterpret the stable intersection number with the red subweb as a stable intersection number with the 3 half D5-branes inside O5$^+$-plane, whichever interpretation gives a consistent magnetic quiver.

Some part of the structure in the magnetic quiver discussed above may be more natural to understand if we consider Hanany-Witten transition. Suppose we concentrate only on the red subweb as well as remaining D5-branes on the O5-planes while omitting the remaining part. By moving three half D7-branes from the right to the left of the red subweb, we obtain a simpler web diagram, from which we can straightforwardly read off most of the SO and the USp gauge nodes in the magnetic quiver. This discussion is parallel to the 5-brane analysis for the Higgs branch of the 5d Sp(N) gauge theory at finite coupling in [1]. This observation would be useful to partially support our magnetic quiver but if we need to obtain the full structure of the magnetic quiver, the original orientifold web would be more convenient.

Finally, to understand if the $\mathbb{Z}_2$ node in the magnetic quiver of Figure 37 is gauge or flavor, we computed the Hilbert series of the Higgs branch in both cases, and compared with the unitary magnetic quiver. We find that only when we take $\mathbb{Z}_2$ node to be gauge, the match is recovered. The Higgs branch Hilbert series reads

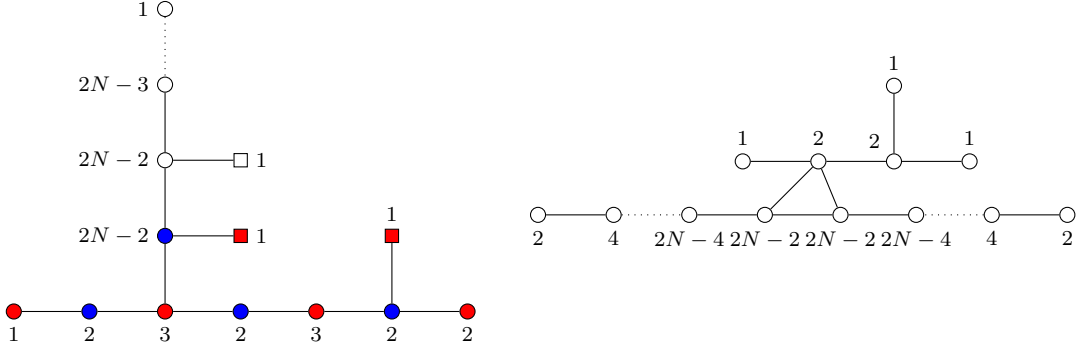$$\mathrm{HS}_H(t^2) = 1 + t^2 + 2t^3 + 5t^4 + 6t^5 + O(t^6). \tag{4.2}$$

Figure 37: Magnetic quivers for the $+_N^{3,1}$ theory.

4.2 The $\tilde{K}_N^1$ theory

The $\tilde{K}_N^1$ theory in the class of O5$^-$-O5$^+$ is obtained from the $+_{N+1}^{3,1}$ theory by decoupling a flavor from (4.1). At low energies, there is a gauge theory description

$$\overbrace{\mathrm{SO}(6) - \mathrm{USp}(2) - \mathrm{SO}(6) - \cdots - \mathrm{USp}(2) - \mathrm{SO}(6) - \mathrm{USp}(2)}^{2N} - [3] \tag{4.3}$$

The orientifold web for the $\tilde{K}_N^1$ theory is presented in Figure 38.

In Figure 34 and Figure 36, the $SU(2N + 1)$ gauge node has $2N + 1$ flavor, and is coupled to a non-Lagrangian theory, where the figures are depicted for the case $N = 1$. Decoupling one flavor from the $SU(2N + 1)$ gauge node, we obtain the web diagrams in Figure 39.
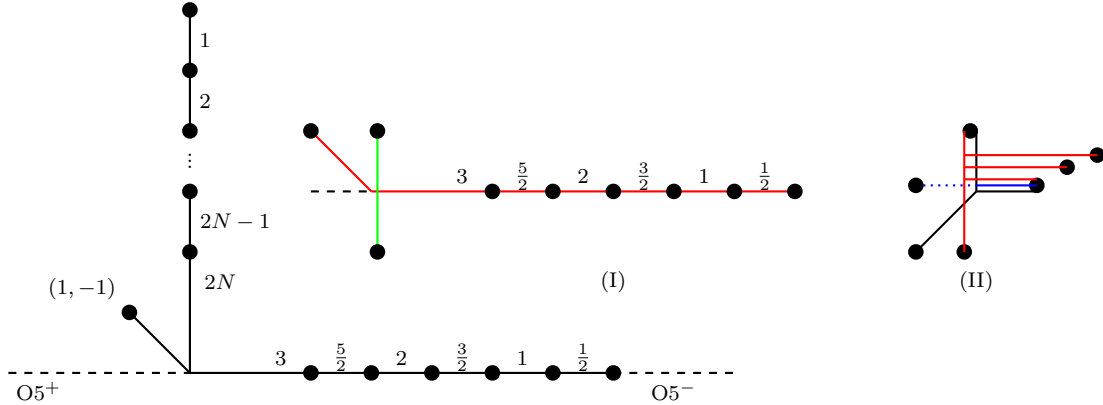

Figure 38: An orientifold web for the $\tilde{K}_N^1$ theory.

The $\tilde{K}_N^1$ theory has two maximal subdivisions, as in Figure 38. In maximal subdivision (I), the red subweb cannot be detached from the O5-plane and thus, giving fundamental hypermultiplets to the USp($2N$) node coming from the $2N$ NS5-branes intersecting with the O5-planes. In maximal subdivision (II), there is a blue dotted line on the O5$^+$-plane

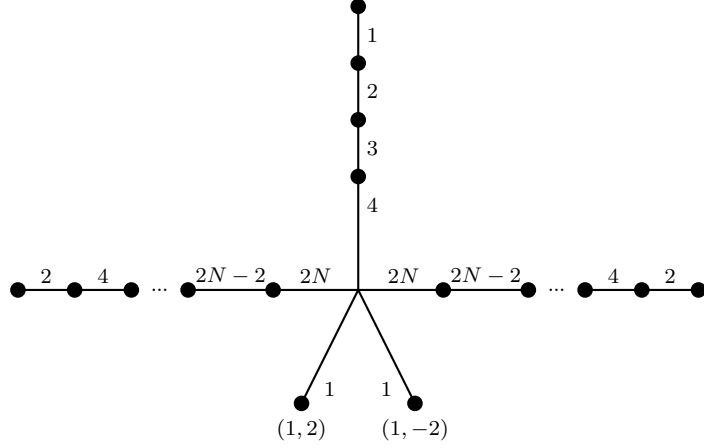**Figure 39**: A unitary web description of the $\tilde{K}_N^1$ theory.

connected to the ordinary blue line on the O5⁻-plane, analogous to the case for the $+_N^{3,1}$ theory. However, this does not become part of a gauge node because there are no other half D5-branes available at the same place. Therefore, both the blue subweb and the red subweb contribute as fundamental hypermultiplets of various gauge nodes. The magnetic quivers are given in Table 14.

To understand if the two $\mathbb{Z}_2$ nodes in the magnetic quiver associated with the maximal subdivision (II) are gauge or flavor, we computed the Hilbert series of the Higgs branch in both cases and compared with the unitary magnetic quiver. We find that only when we take both $\mathbb{Z}_2$ nodes to be flavor, the match is recovered. The Higgs branch Hilbert series reads

$$\mathrm{HS}_H(t^2) = 1 + 5t^2 + 8t^3 + 18t^4 + 36t^5 + 71t^6 + 120t^7 + \cdots. \tag{4.4}$$

The Coulomb branch Hilbert series is tabulated in Table 15.

Table 14: Magnetic quivers for various maximal subdivisions (MS) of the $\tilde{K}_N^1$ theory.

MS	Unitary magnetic quiver $\mathrm{HS}(t)$	Orthosymplectic magnetic quiver $\mathrm{HS}(t; \vec{m} \in \mathbb{Z})$	$\mathrm{HS}(t; \vec{m} \in \mathbb{Z}+\frac{1}{2})$
$(\mathrm{I})_{N=1}$	$\dfrac{1 + t + 2t^2 + t^3 + t^4}{(1 - t)^4 (1 + t)^2}$ $= 1 + 3t + 9t^2 + 18t^3$ $+35t^4 + 57t^5 + \cdots$	$\dfrac{1 + t + 2t^2 + t^3 + t^4}{(1 - t)^4 (1 + t)^2}$ $= 1 + 3t + 9t^2 + 18t^3$ $+35t^4 + 57t^5 + \cdots$	not required
$(\mathrm{I})_{N=2}$	$1 + 15t + 135t^2 + 888t^3 + 4709t^4 +$ $21144t^5 + \cdots$	$1 + 15t + 135t^2 + 888t^3 + 4709t^4 +$ $21144t^5 + \cdots$	not required
$(\mathrm{II})_{N=1}$	$1 + 19t + 173t^2 + 24t^{5/2} +$ $1042t^3 + 328t^{7/2} + 4760t^4 +$ $2312t^{9/2} + 17908t^5 + \cdots$	$1 + 19t + 173t^2 + 24t^{5/2} +$ $1042t^3 + 328t^{7/2} + 4760t^4 +$ $2312t^{9/2} + 17908t^5 + \cdots$	not required
$(\mathrm{II})_{N=2}$	$1 + 31t + 495t^2 + 5443t^3 + 48t^{7/2} +$ $46260t^4 + 1472t^{9/2} + 323154t^5 + \cdots$	$1 + 31t + 495t^2 + 5443t^3 + 48t^{7/2} +$ $46260t^4 + 1472t^{9/2} + 323154t^5 + \cdots$	not required

Table 15: Coulomb branch Hilbert series for the unitary and orthosymplectic magnetic quivers presented in Table 14 for the $\tilde{K}_N^1$ theory.

5 Magnetic quivers from $\widetilde{\mathrm{O5}}^+$

Finally we consider some examples where we have an $\widetilde{\mathrm{O5}}^+$-plane on one or two of the ends in the orientifold web configuration.

5.1 $\widetilde{\mathrm{O5}}^+$ - $\widetilde{\mathrm{O5}}^+$

We begin with an example where we have $\widetilde{\mathrm{O5}}^+$-planes on the two ends of the brane configuration. For constructing such a configuration we start from the theory considered in section 3.1, which yields the orthosymplectic quiver (3.1) as an IR theory. From the quiver theory (3.1), we Higgs the two $SO(6)$ gauge theories on the ends. The resulting IR theory becomes

$$
\overbrace{SO(5) - \mathrm{USp}(2) - SO(6) - \mathrm{USp}(2) - SO(6) - \cdots - \mathrm{USp}(2) - SO(6) - \mathrm{USp}(2) - SO(5)}^{2N-1}
$$

with $\left[\tfrac{1}{2}\right]$ attached below the first $\mathrm{USp}(2)$ and $\left[\tfrac{1}{2}\right]$ attached below the last $\mathrm{USp}(2)$.

$$\tag{5.1}$$

where $\frac{1}{2}$ represents a half-hypermultiplet in the fundamental representation of $\mathrm{USp}(2)$. It is possible to construct the corresponding orientifold web diagram by performing the same Higgsing to the web in Figure 23. The orientifold web diagram is depicted in Figure 40 which has asymptotically $\widetilde{\mathrm{O5}}^+$-planes. From the orientifold web configuration the presence of a half D7-brane accounts for the half-hypermultiplet.

The theory in (5.1) can also be constructed by gluing 2 copies of $SO(5)$ with 1 vector and 1 singlet, and $N - 2$ copies of $SO(6)$ with two vectors via successive gauging of $\mathrm{USp}(2)$ subgroup of the global symmetry. This allows us to propose a unitary web in Figure 40 by gluing together 2 copies of $\mathrm{USp}(4)$ with one antisymmetric hypermultiplet and one singlet,

and $N-2$ copies of $SU(4)_0$ with two antisymmetric hypermultiplets via gauging $SU(2)$ subgroups of the global symmetry.
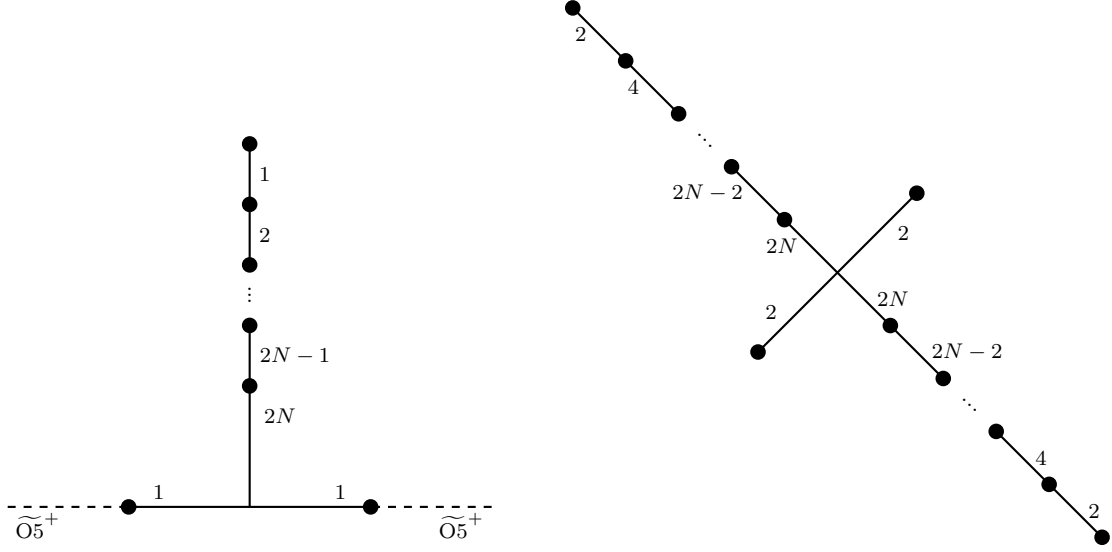

Figure 40: Orientifold web(left), and ordinary web(right) for the $+_N$ theory. The maximal subdivision is the trivial one and therefore not shown explicitly.

The orthosymplectic and unitary magnetic quiver theories can be read off from the web diagrams in Figure 40, and they are given in Figure 41. The corresponding Coulomb branch Hilbert series are given in Table 16.
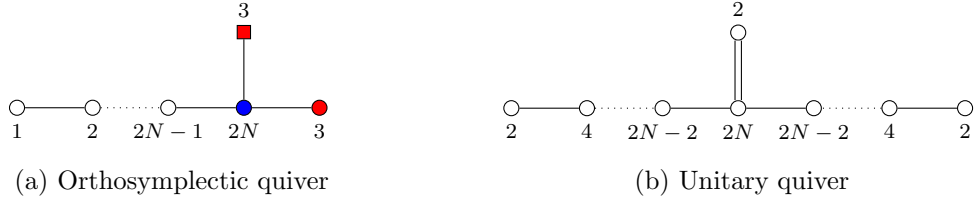

(a) Orthosymplectic quiver

(b) Unitary quiver

Figure 41: Magnetic quivers for the $+_N$ theory

$+_N$	Unitary magnetic quiver $HS(t)$	Orthosymplectic magnetic quiver	
		$HS(t; \vec{m} \in \mathbb{Z})$	$HS(t; \vec{m} \in \mathbb{Z} + \frac{1}{2})$
$+_1$	bad theory	bad theory	not required
$+_2$	$1 + 16t + 168t^2 + 1315t^3 +$ $8329t^4 + 44491t^5 + \cdots$	$1 + 16t + 168t^2 + 1315t^3 +$ $8329t^4 + 44491t^5 + \cdots$	not required

Table 16: Coulomb branch Hilbert series for the unitary and orthosymplectic magnetic quivers presented in Figure 41 for the $+_N$ theory.
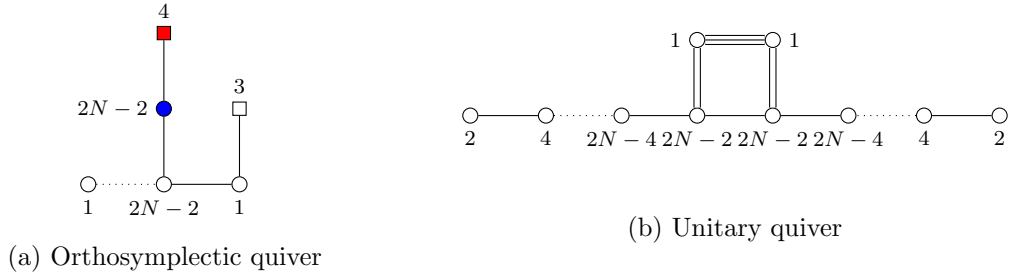
5.2 $\widetilde{O5}^+$ - $O5^+$

It is also possible to consider an example where we have an $\widetilde{O5}^+$-plane on one end and an $O5^+$-plane on the other end. We again start from the theory considered in section 3.1, which yields the orthosymplectic quiver (3.1) as an IR theory. From the quiver theory (3.1), we Higgs the $SO(6)$ gauge theory on the right end and decouple flavor from the $SO(6)$ gauge on the left end. Then the resulting IR theory becomes

$$[1] - \overbrace{SO(6) - USp(2) - SO(6) - \cdots - SO(6) - USp(2) - SO(5)}^{2N-1} \tag{5.2}$$
$$\underset{\left[\frac{1}{2}\right]}{|}$$

We can construct the corresponding orientifold web diagram by performing the same Higgsing and the decoupling to the web in Figure 23. The orientifold web diagram is depicted in Figure 42 which has asymptotically an $\widetilde{O5}^+$-plane and an $O5^+$-plane.

This theory in (5.2) can also be made by gluing 1 copy of $SO(5)$ with 1 vector and 1 singlet, and $N-1$ copies of $SO(6)$ with two vectors via successive gauging of $USp(2)$ subgroup of the global symmetry. This allows us to propose the corresponding unitary web in Figure 42 by gluing together 1 copy of $USp(4)$ with one antisymmetric hypermultiplet and one singlet, and $N-1$ copies of $SU(4)_0$ with two antisymmetric hypermultiplets via gauging $SU(2)$ subgroups of the global symmetry.

Figure 42: Orientifold and unitary web diagram for the κ_N^1 theory.

The orthosymplectic and unitary magnetic quiver theories can be read off from the web diagrams in Figure 42, and they are given in Figure 43. The corresponding Coulomb branch Hilbert series is presented in Table 17.

(a) Orthosymplectic quiver

(b) Unitary quiver

Figure 43: Magnetic quivers for the κ_N^1 theory

K_N^1	Unitary magnetic quiver	Orthosymplectic magnetic quiver	
	HS(t)	HS($t; \vec{m} \in \mathbb{Z}$)	HS($t; \vec{m} \in \mathbb{Z}+\frac{1}{2}$)
K_2^1	$1 + 9t + 53t^2 + 6t^{5/2} + 227t^3 +$ $60t^{7/2} + 792t^4 + 318t^{9/2} + 2358t^5$	$1 + 9t + 53t^2 + 6t^{5/2} + 227t^3 +$ $60t^{7/2} + 792t^4 + 318t^{9/2} + 2358t^5$	not required
K_3^1	$1 + 25t + 349t^2 + 3499t^3 + \cdots$	$1 + 25t + 349t^2 + 3499t^3 + \cdots$	not required

Table 17: Coulomb branch Hilbert series for the unitary and orthosymplectic magnetic quivers presented in Figure 43 for the κ_N^1 theory.

6 Conclusion

In this paper, we studied infinite coupling Higgs branches of 5d superconformal theories based on 5-brane webs, by constructing 3d magnetic quivers whose Coulomb branch yields the Higgs branch of the 5d system. Our primary focus was 5d theories, which can be engineered by 5-brane webs with O5-planes and also without O5-planes by either S-duality or some gauging subalgebra of flavor symmetry. As a 5-brane web without an O5-plane gives a unitary magnetic quiver, while that with an O5-plane gives an orthosymplectic magnetic quiver, these 5d theories of two different 5-brane web descriptions should yield the same Higgs branch. In other words, the Coulomb branches from the corresponding unitary and orthosymplectic magnetic quivers should agree. We employed this fact to further develop how to construct orthosymplectic magnetic quivers [1] by comparing the counterpart unitary magnetic quiver, in particular, by explicitly checking the Hilbert series for both magnetic quivers. With various decoupling limits for both 5-brane webs with/without O5-planes, we proposed a generalization of the rules for constructing 3d magnetic quivers from 5-brane webs with O5-planes. The novel features that we found include (i) generalized stable intersection number involving subwebs intersecting with its mirror through an O5-plane as well as the stable intersection with an O5-plane, which in turn determines the number of charge 2 matter appearing in the magnetic quivers, (ii) a new type of hypermultiplet transforming in the fundamental-fundamental representation of two gauge nodes, (iii) appearance of matter in the antisymmetric representation of gauge nodes. (iv) possibility of decomposable and not-decomposable for seeming equivalent subwebs depending the discrete theta angles for 5-brane configurations for 5d USp gauge groups, and (v) $\mathbb{Z}_2$ gauge nodes.

We also checked the matching of both the Coulomb branch and the Higgs branch Hilbert series for all the unitary and orthosymplectic magnetic quivers appearing in this work (though we provided the Higgs branch Hilbert series only when it was required). Having checked that each pair of unitary and orthosymplectic magnetic quivers have isomorphic Coulomb and Higgs branch moduli space of vacua, it is natural to suggest a possible duality between each pair. It would be interesting to check this duality more systematically, for instance, via superconformal indices or partition functions. In fact, we checked the partition functions for some 3d theories and found that their partition functions can be mapped to each other by a simple fugacity map. Understanding the 4d origin of this duality, should it exist, would be another exciting direction to pursue.

Though our construction applies to generic 5d theories of any rank, some lower rank theories possess special dualities [39]. In particular, 5-brane webs for most of rank 2 superconformal theories have been constructed [23], a systematic study of their magnetic quivers would also shed some light on a better understanding of orthosymplectic magnetic quivers [54]. Some magnetic quivers of the rank 2 theories were also considered in [51, 55, 56].

Acknowledgments

A Hilbert series computations

A.1 Coulomb branch Hilbert series

Here we briefly review the computation of the Hilbert series of the Coulomb branch of the moduli space for the 3d $\mathcal{N} = 4$ quiver theories. For the computation, we use the *monopole formula* prescribed in [57] which essentially counts the number of *dressed* monopole operators according to their conformal dimension. We refer the readers to [57] for the technical details of the formula and simply quote the result here:

$$\text{HS}_C(t) = \sum_{\vec{m}_1} \sum_{\vec{m}_2} \ldots \sum_{\vec{m}_x} t^{\Delta(\vec{m}_1, \ldots, \vec{m}_x)} \prod_{i=1}^{x} P_{G_i}(t, \vec{m}_i) \; . \tag{A.1}$$

Let us briefly explain various terms in this formula. The gauge group of the theory under consideration is $G_1 \times G_2 \times \ldots \times G_x$, where each of the group G_i is indicated as a circular node in the quiver description. For a particular group G in the quiver, the monopole operators are specified by the magnetic fluxes $\vec{m} = (m_1, m_2, \ldots m_r)$ which belong to the weight lattice $\Gamma(\hat{G})$ of $\hat{G}$, the GNO (or Langlands) dual group of G (r being the rank of G or $\hat{G}$). The gauge invariant monopole operators are specified by those $\vec{m}$ which take values in the quotient space:

$$\vec{m} \in \Gamma(\hat{G})/W(\hat{G}) , \tag{A.2}$$

where $W(\hat{G})$ is the Weyl group of $\hat{G}$. These are precisely the fluxes which contribute in the summation in the monopole formula (A.1). The Langland duals and the associated magnetic fluxes for some of the Lie groups are given below:

G	$\hat{G}$	$\vec{m} \in \Gamma(\hat{G})/W(\hat{G})$
U(r)	U(r)	$m_1 \geq m_2 \geq \ldots \geq m_r \geq -\infty$
SO($2r+1$)	USp($2r$)	$m_1 \geq m_2 \geq \ldots \geq m_r \geq 0$
USp($2r$)	SO($2r+1$)	$m_1 \geq m_2 \geq \ldots \geq m_r \geq 0$
SO($2r$)	SO($2r$)	$m_1 \geq m_2 \geq \ldots \geq |m_r| \geq 0$

$$\tag{A.3}$$

The factor $P_G(t, \vec{m})$ is the classical dressing function which counts the gauge invariants of the residual gauge group which is left unbroken by the magnetic flux $\vec{m}$, according to their dimension, and is given as,

$$P_G(t, \vec{m}) = \prod_{i=1}^{r} \frac{1}{1 - t^{d_i(\vec{m})}} , \tag{A.4}$$

where $d_i(\vec{m})$ are the degrees of Casimir invariants of the unbroken residual gauge group. These functions can be written in a computationally friendly manner by collecting the fluxes which are equal in $\vec{m}$. To do this, let us define an auxiliary sequence of non-increasing fluxes in $\vec{m}$, which we shall denote as $\vec{n} = (n_1, n_2, \ldots, n_r)$. We collect all the repeating fluxes together and define $\vec{n}_{\mathrm{res}} = (a_1^{r_1}, \ldots, a_u^{r_u})$ where the notation $a_i^{r_i}$ means that the integer a_i is repeated r_i times (where $r_1 + \ldots + r_u = r$). The dressing functions can now be defined for various groups as:

G	$\vec{n} = (n_1, n_2, \ldots, n_r)$	$\vec{n}_{\mathrm{res}}$	P_G
U(r)	$(m_1, m_2, \ldots, m_r)$	$(a_1^{r_1}, \ldots, a_u^{r_u})$	$\prod_{i=1}^{u} \prod_{k=1}^{r_i} \frac{1}{1-t^k}$
SO($2r+1$)	$(m_1, m_2, \ldots, m_r)$	$(a_1^{r_1}, \ldots, a_{u-1}^{r_{u-1}}, 0^{r_u})$	$A(r_u) \left(\prod_{i=1}^{u-1} \prod_{k=1}^{r_i} \frac{1}{1-t^k} \right)$
USp($2r$)	$(m_1, m_2, \ldots, m_r)$	$(a_1^{r_1}, \ldots, a_{u-1}^{r_{u-1}}, 0^{r_u})$	$A(r_u) \left(\prod_{i=1}^{u-1} \prod_{k=1}^{r_i} \frac{1}{1-t^k} \right)$
SO($2r$)	$(m_1, m_2, \ldots, |m_r|)$	$(a_1^{r_1}, \ldots, a_{u-1}^{r_{u-1}}, 0^{r_u})$	$B(r_u) \left(\prod_{i=1}^{u-1} \prod_{k=1}^{r_i} \frac{1}{1-t^k} \right)$

$$\tag{A.5}$$

where the factors $A(r_u)$ and $B(r_u)$ are explicitly dependent on the number of vanishing fluxes and are given as,

$$A(j) = \prod_{k=1}^{j} \frac{1}{1 - t^{2k}} \quad ; \quad B(j) = \delta_{j0} + \left(\frac{1}{1 - t^j} \prod_{k=1}^{j-1} \frac{1}{1 - t^{2k}} \right) (1 - \delta_{j0}) . \tag{A.6}$$

The last thing we need in the monopole formula (A.1) is the R-charge or the conformal dimension $\Delta(\vec{m}_1, \ldots, \vec{m}_x)$ of the bare monopole operators associated with various gauge groups in the quiver specified by the GNO magnetic fluxes $\vec{m}_1, \ldots, \vec{m}_x$. The conformal dimension gets contribution from the vector multiplets and the hyper multiplets present in the theory:

$$\Delta = \Delta_{\text{vector}} + \Delta_{\text{hyper}} . \tag{A.7}$$

These contributions are given as follows. Consider a node with group G in the quiver and denote α to be a positive root of G. The vector contribution is computed as,

$$\Delta_{\text{vector}}(\vec{m}) = - \sum_{\alpha \in \Delta_+} |\alpha(\vec{m})| , \tag{A.8}$$

where the positive roots of G act on the GNO fluxes $\vec{m}$ associated with the weight lattice of GNO dual group $\hat{G}$ and the sum is taken over all positive roots of G. By restricting these fluxes to the fundamental Weyl chamber, the above sum can be explicitly performed and is given as,

G	$\Delta_+(G)$	$\Delta_{\text{vector}}(\vec{m})$
U(r)	$\{e_i - e_j\}_{1 \leq i < j \leq r}$	$-\sum_{k=1}^{r}(r + 1 - 2k)m_k$
SO$(2r+1)$	$\{e_i - e_j, e_i + e_j, e_i\}_{1 \leq i < j \leq r}$	$-\sum_{k=1}^{r}(2r + 1 - 2k)m_k$
USp$(2r)$	$\{e_i - e_j, e_i + e_j, 2e_i\}_{1 \leq i < j \leq r}$	$-\sum_{k=1}^{r}(2r + 2 - 2k)m_k$
SO$(2r)$	$\{e_i - e_j, e_i + e_j\}_{1 \leq i < j \leq r}$	$-\sum_{k=1}^{r-1}(2r - 2k)m_k$

$$\tag{A.9}$$

Once we compute this vector term for individual nodes in the quiver, we can simply add them to get the full vector contribution:

$$\Delta_{\text{vector}}(\vec{m}_1, \ldots, \vec{m}_x) = \sum_{i=1}^{x} \Delta_{\text{vector}}(\vec{m}_i) . \tag{A.10}$$

The term Δ_{hyper} is the contribution of hypermultiplets (the links connecting the nodes in the quiver diagram) present in the theory which is given as the sum over the weights of the matter field representation under the gauge groups. To write an explicit formula in terms of the GNO fluxes, consider a hypermultiplet connecting two groups G_r and G_s of ranks r and s:

$$\tag{A.11}$$

Further consider the GNO fluxes associated with the two groups as $\vec{a} = (a_1, a_2, \ldots, a_r)$ and $\vec{b} = (b_1, b_2, \ldots, b_s)$. The weights associated with the fundamental representation of the two groups can be written as a tuple of GNO fluxes which we denote as $w(\vec{a})$ and $w(\vec{b})$. For the classical Lie groups, they are given below:

G	$\vec{m}$	$w(\vec{m})$
U(r)	$(m_1, \ldots, m_r)$	$(m_1, \ldots, m_r)$
SO$(2r+1)$	$(m_1, \ldots, m_r)$	$(m_1, \ldots, m_r, 0, -m_r, \ldots, -m_1)$
USp$(2r)$	$(m_1, \ldots, m_r)$	$(m_1, \ldots, m_r, -m_r, \ldots, -m_1)$
SO$(2r)$	$(m_1, \ldots, m_r)$	$(m_1, \ldots, m_r, -m_r, \ldots, -m_1)$

$$\tag{A.12}$$

The hypermulitplet contribution is now easy to write. If we denote $w_i(\vec{m})$ to be the ith component in $w(\vec{m})$, the contribution is:

$$
\Delta_{\text{hyper}}\left(\vec{a},\vec{b}\right) = \begin{cases} \dfrac{1}{4} \sum_i \sum_j \left| w_i(\vec{a}) - w_j(\vec{b}) \right| , & \text{when } G_r/G_s = \text{SO/USp or USp/SO} \\[4mm] \dfrac{1}{2} \sum_i \sum_j \left| w_i(\vec{a}) - w_j(\vec{b}) \right| , & \text{otherwise} \end{cases} ,
$$

$$(A.13)$$

where a hypermultiplet comes with a 1/2 factor and a half-hypermultiplet (the link connecting a SO type of node to USp type of node) comes with a 1/4 factor in the conformal dimension. Summing over the contributions of all the hypermultiplets present in the theory will finally give the Δ_{hyper} for the full quiver. There can also be flavor symmetry groups associated with a gauge group. Such groups are denoted by a square node in the quiver. The GNO fluxes for such nodes are all 0 ($\vec{m} = 0$) and they do not contribute to Δ_{vector} in the conformal dimension. The contribution of the link connecting the gauge node with a flavor node can be obtained by simply computing Δ_{hyper} as usual and then setting the fluxes of GNO dual to 0:

$$
\boxed{G_r} \longrightarrow \boxed{G_s} \quad \implies \quad \Delta_{\text{hyper}} = \Delta_{\text{hyper}}\left(\vec{a},\vec{0}\right) . \tag{A.14}
$$

We may also encounter the cases where we need to put multiple links between two nodes in the quiver. In this scenario, the contribution of the individual links are simply added up. For example, in case of triple hypers, we have:

$$
\left(G_r\right) \equiv \equiv \left(G_s\right) \quad \implies \quad \Delta_{\text{hyper}} = 3 \times \Delta_{\text{hyper}}\left(\vec{a},\vec{b}\right) . \tag{A.15}
$$

We have also proposed an exotic hypermultiplet which transforms under the fundamental-fundamental representations of the unitary gauge nodes it connects. We denote this exotic hyper by a dashed line in the quiver between the two unitary nodes. The contribution of such a hyper to the conformal dimension is given as:

$$
\left(\text{U}(r)\right) \dashv \dashv \dashv \left(\text{U}(s)\right) \quad \implies \quad \Delta_{\text{hyper}} = \frac{1}{2} \sum_{i=1}^{r} \sum_{j=1}^{s} \left| w_i(\vec{a}) + w_j(\vec{b}) \right| , \tag{A.16}
$$

where $\vec{a}$ and $\vec{b}$ are the GNO fluxes of the two nodes.

A.2 Higgs branch Hilbert series

The Hilbert series of the Higgs branch of a 3d $\mathcal{N} = 4$ theory can be easily computed. Suppose the gauge group is G, and the matter content is given by N_h hypermultiplets charged under representations R_i ($i = 1, \ldots, N_h$) of the gauge group, and possibly charged under representations R_i' of the flavor group. The Hilbert series is then schematically given by

$$\text{HS}(t) = \int_G d\mu_G \; \text{Pfc}(w,t) \text{PE} \left[\sum_{i=1}^{2N_h} \text{char}_{R_i}(w) \, \text{char}_{R_i'}(x) t^{\frac{1}{2}} \right] \tag{A.17}$$

Let us now review the various terms entering in equation (A.17).

The term

$$\text{PE} \left[\sum_{i=1}^{2N_h} \text{char}_{R_i}(w) \, \text{char}_{R_i'}(x) t^{\frac{1}{2}} \right] \tag{A.18}$$

is generating all the possible symmetrized product of all the scalars inside the hypermultiplets. Here $w = (w_1, \cdots, w_r)$ is a collective variable denoting the fugacities of the rank r gauge group, and $x = (x_1, \cdots, x_r)$ are fugacities of the flavor group. Notice that these fugacities take value in the gauge (resp. flavor) symmetry group. Therefore each of the x and w is a complex phase. The fugacity t is a fugacity counting the conformal dimension. The exponent of t is $\frac{1}{2}$ as this is the conformal dimension of one free scalar in 3d. The term $\text{char}_{R_i}(w)$ (resp. $\text{char}_{R_{i_i}}(x)$) is the character of the representation under the gauge group (resp. flavor group) under which the i-th hypermultiplet is charged. The function $\text{PE}[\cdot]$ is the plethystic exponential, defined as

$$\text{PE}[f(x)] := \exp \left(\sum_{k=1}^{\infty} \frac{1}{k} f\left(x^k \right) \right) \tag{A.19}$$

for any function $f(x)$ such that $f(0) = 0$. The term $\text{Pfc}(w,t)$ is a prefactor, encoding the fact that the symmetrized product of the scalars are not all independent, but they obey some relationships coming from the F-term constraints. This prefactor term is given by

$$\text{Pfc}(w,t) = \text{PE} \left[\sum_{i=1}^{N_r} \text{char}_{R_i''}(w) t^{d_i} \right]^{-1} \tag{A.20}$$

where $\text{char}_{R_i''}(w)$ is the character of the representation of the i-th relation, and d_i its degree in conformal dimension. Given the constrained structure of the superpotential in theories with 8 supercharges, typically $\text{char}_{R_i''}(w)$ will be the character of the adjoint, and the relation will appear at quadratic order in the scalars: $d_i = 1$. Finally, the integral over the gauge group is performed in order to count only gauge invariant operators, and not just all the symmetric products of scalars modulo the F-term constraint. Such integral is called the Molien integral. The integration measure μ_G is given, for any continuous gauge group as

$$\int_G d\mu_G = \frac{1}{(2\pi i)^r} \oint_{|w|_1=1} \cdots \oint_{|w|_r=1} \frac{dw_1}{w_1} \cdots \frac{dw_r}{w_r} \prod_{\alpha \in \Delta^+} \left(1 - \prod_{k=1}^{r} w_k^{\alpha_k} \right) \tag{A.21}$$

where Δ^+ is the set of the positive roots of the Lie algebra of G. Notice that despite the integral is formally performed over the full gauge group, the use of the Molien measure localizes the integral just on the Cartan torus. Every fugacity w_i is then integrated just

on the unit circle. The factor $\frac{dw_r}{w_r}\prod_{\alpha \in \Delta^+}\left(1 - \prod_{k=1}^r w_k^{\alpha_k}\right)$ can be thought of the Jacobian for the change of variable recasting the integral over the gauge group into the integral over the its Cartan torus.

The procedure outlined above can be slightly modified if discrete gauge groups are present. Let us call the discrete gauge group H, and its order $|H|$. We can introduce a fugacity z for the discrete gauge symmetry, valued now in H. The term generating all the symmetrized products of scalars will now read

$$\mathrm{PE}\left[\sum_{i=1}^{2N_h}\mathrm{char}_{R_i}(w)\,\mathrm{char}_{R_i'}(x)zt^{\frac{1}{2}}\right] \tag{A.22}$$

and there will be no prefactor contribution. This is consistent with the fact that there is no vector multiplet associated to a discrete gauge factor, therefore there will be no F-term relations for it. To only retain the singlets for the discrete factor, the Molien integral over H still has to be performed. However, since now the z fugacity takes values is a discrete group, the integral over all the elements of the gauge group is now replaced with discrete sum:

$$\int_H d\mu_H \mathrm{Pfc}(w,t)\mathrm{PE}\left[\sum_{i=1}^{2N_h}\mathrm{char}_{R_i}(w)\,\mathrm{char}_{R_i'}(x)zt^{\frac{1}{2}}\right] =$$

$$= \frac{1}{|H|}\mathrm{Pfc}(w,t)\sum_h^{|H|}\mathrm{PE}\left[\sum_{i=1}^{2N_h}\mathrm{char}_{R_i}(w)\,\mathrm{char}_{R_i'}(x)zt^{\frac{1}{2}}\right]_{|z=h} \tag{A.23}$$

After performing all the discrete Molien integrations for all the discrete factors of the gauge group, the integrations on the continuous factors still have to be performed, using eq (A.21).

B Palindromic polynomials

We summarize in Table 18 explicit forms of parlindromic polynomials which arise in the computation of the Hilbert series of Coulomb branches of some theories discussed in section 2 and section 3.

Label	Polynomial
$P_0(t)$	$1 + 98t + 3312t^2 + 53305t^3 + 468612t^4 + 2421286t^5 + 7664780t^6 + 15203076t^7 + 19086400t^8 + 15203076t^9 + 7664780t^{10} + 2421286t^{11} + 468612t^{12} + 53305t^{13} + 3312t^{14} + 98t^{15} + t^{16}$
$P_1(t)$	$1 + 52t + 2669t^2 + 63963t^3 + 1011274t^4 + 11000351t^5 + 88762624t^6 + 549522302t^7 + 2698733098t^8 + 10730180908t^9 + 35179028314t^{10} + 96291284692t^{11} + 222448351508t^{12} + 436990904921t^{13} + 734668194786t^{14} + 1061421775571t^{15} + 1322191150030t^{16} + 1422261110352t^{17} + \ldots \text{palindrome} \ldots + 52t^{33} + t^{34}$
$P_2(t)$	$64t + 2560t^2 + 64768t^3 + 1006592t^4 + 11022656t^5 + 88672768t^6 + 549832576t^7 + 2697805824t^8 + 10732603264t^9 + 35173452800t^{10} + 96302654592t^{11} + 222427719168t^{12} + 437024347328t^{13} + 734619634688t^{14} + 1061485070080t^{15} + 1322116993536t^{16} + 1422339277952t^{17} + \ldots \text{palindrome} \ldots + 2560t^{32} + 64t^{33}$
$P_3(t)$	$1 + 31t + 231t^2 + 595t^3 + 595t^4 + 231t^5 + 31t^6 + t^7$
$P_4(t)$	$1 + 22t + 245t^2 + 1442t^3 + 5355t^4 + 12978t^5 + 21919t^6 + 25900t^7 + 21919t^8 + 12978t^9 + 5355t^{10} + 1442t^{11} + 245t^{12} + 22t^{13} + t^{14}$
$P_5(t)$	$1 + 14t + 91t^2 + 336t^3 + 819t^4 + 1362t^5 + 1618t^6 + 1362t^7 + 819t^8 + 336t^9 + 91t^{10} + 14t^{11} + t^{12}$
$P_6(t)$	$1 + 12t + 58t^2 + 124t^3 + 170t^4 + 124t^5 + 58t^6 + 12t^7 + t^8$
$P_7(t)$	$8t + 48t^2 + 136t^3 + 176t^4 + 136t^5 + 48t^6 + 8t^7$
$P_8(t)$	$1 + 6t + 44t^2 + 146t^3 + 446t^4 + 826t^5 + 1343t^6 + 1436t^7 + 1343t^8 + 826t^9 + 446t^{10} + 146t^{11} + 44t^{12} + 6t^{13} + t^{14}$
$P_9(t)$	$1 + 6t + 35t^2 + 108t^3 + 407t^4 + 1014t^5 + 2720t^6 + 5198t^7 + 10773t^8 + 16712t^9 + 27493t^{10} + 35046t^{11} + 47571t^{12} + 50460t^{13} + 56752t^{14} + 50640t^{15} + 47571t^{16} + 35046t^{17} + 27493t^{18} + 16712t^{19} + 10773t^{20} + 5198t^{21} + 2720t^{22} + 1014t^{23} + 407t^{24} + 108t^{25} + 35t^{26} + 6t^{27} + t^{28}$
$P_{10}(t)$	$16t^2 + 80t^3 + 368t^4 + 960t^5 + 2704t^6 + 5296t^7 + 10912t^8 + 16832t^9 + 27728t^{10} + 35184t^{11} + 47344t^{12} + 50192t^{13} + 56608t^{14} + 50192t^{15} + 47344t^{16} + 35184t^{17} + 27728t^{18} + 16832t^{19} + 10912t^{20} + 5296t^{21} + 2704t^{22} + 960t^{23} + 368t^{24} + 80t^{25} + 16t^{26}$
$P_{11}(t)$	$1 + 11t + 57t^2 + 170t^3 + 324t^4 + 398t^5 + 324t^6 + 170t^7 + 57t^8 + 11t^9 + t^{10}$
$P_{12}(t)$	$1 + 3t + 38t^2 + 69t^3 + 225t^4 + 240t^5 + 372t^6 + 240t^7 + 225t^8 + 69t^9 + 38t^{10} + 3t^{11} + t^{12}$
$P_{13}(t)$	$8t + 20t^2 + 112t^3 + 156t^4 + 328t^5 + 276t^6 + 328t^7 + 156t^8 + 112t^9 + 20t^{10} + 8t^{11}$
$P_{14}(t)$	$1 + 2t + 6t^2 + 10t^3 + 22t^4 + 26t^5 + 39t^6 + 36t^7 + 39t^8 + 26t^9 + 22t^{10} + 10t^{11} + 6t^{12} + 2t^{13} + t^{14}$
$P_{15}(t)$	$1 - 2t^2 + 8t^{5/2} + t^3 - 8t^{7/2} + t^4 - 8t^{9/2} + 13t^5 + 8t^{11/2} - 24t^6 - 5t^7 + 8t^{15/2} + 15t^8 - 24t^{17/2} - t^9 + 8t^{19/2} + 9t^{10} + 8t^{21/2} - 16t^{11} + 8t^{23/2} + 9t^{12} + 8t^{25/2} - t^{13} - 24t^{27/2} + 15t^{14} + 8t^{29/2} - 5t^{15} - 24t^{16} + 8t^{33/2} + 13t^{17} - 8t^{35/2} + t^{18} - 8t^{37/2} + t^{19} + 8t^{39/2} - 2t^{20} + t^{22}$
$P_{16}(t)$	$1 - 2t^2 + t^3 + t^4 + 16t^5 - 24t^6 - 11t^7 + 18t^8 + 2t^9 + 51t^{10} - 88t^{11} - 12t^{12} + 47t^{13} + 15t^{14} + 62t^{15} - 144t^{16} + 23t^{17} + 44t^{18} + 44t^{19} + 23t^{20} - 144t^{21} + 62t^{22} + 15t^{23} + 47t^{24} - 12t^{25} - 88t^{26} + 51t^{27} + 2t^{28} + 18t^{29} - 11t^{30} - 24t^{31} + 16t^{32} + t^{33} + t^{34} - 2t^{35} + t^{37}$
$P_{17}(t)$	$1 - t - t^2 + t^3 + 4t^5 - 6t^6 - 2t^7 + 4t^8 + t^9 + 7t^{10} - 15t^{11} + t^{12} + 6t^{13} + 4t^{14} + 6t^{15} - 20t^{16} + 6t^{17} + 4t^{18} + 6t^{19} + t^{20} - 15t^{21} + 7t^{22} + t^{23} + 4t^{24} - 2t^{25} - 6t^{26} + 4t^{27} + t^{29} - t^{30} - t^{31} + t^{32}$
$P_{18}(t)$	$1 + 8t + 40t^2 + 107t^3 + 199t^4 + 234t^5 + 199t^6 + 107t^7 + 40t^8 + 8t^9 + t^{10}$
$P_{19}(t)$	$1 + 2t + 6t^2 + 10t^3 + 22t^4 + 26t^5 + 39t^6 + 36t^7 + 39t^8 + 26t^9 + 22t^{10} + 10t^{11} + 6t^{12} + 2t^{13} + t^{14}$

Table 18: Palindromic polynomials appearing in the main sections.

C   More on the number of charge 2 hypermultiplets

In section 2.2, we observed that the number of charge 2 hypermultiplets may be given by (2.6). So far, we have encountered the cases which involve a $(p, 1)$ 5-brane or a $(1, q)$ 5-brane for the origin of charge 2 hypermultiplets. We here give more support for (2.6) by

checking further new examples that involve a (p, q) 5-brane with both p and q larger than 1. In order to consider such examples, we use 5-brane web diagrams whose corresponding orthosymplectic magnetic quiver theories do not have a unitary counterpart. However, we can still check the validity of the 3d orthosymplectic magnetic quivers by comparing their Higgs branch dimension with the dimension of the Coulomb branch moduli space of the original 5d theories.

The first example we consider is the 5d theory realized on the 5-brane web diagram in Figure 44. The central gauge theory is an $SO(4k + 2)$ gauge theory and the diagram has
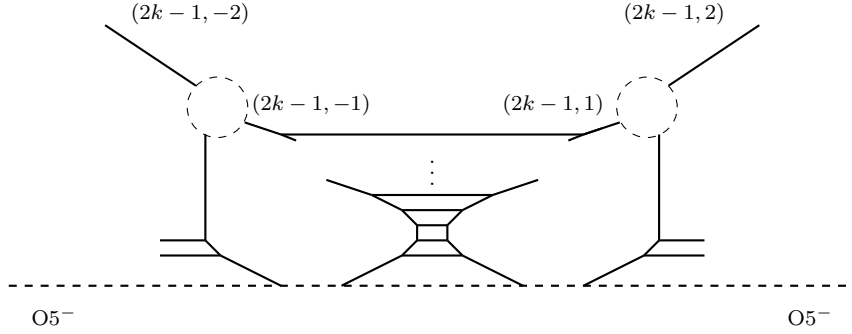
Figure 44: The 5-brane web diagram which has an external $(2k - 1, 2)$ 5-brane and an external $(2k - 1, -2)$ 5-brane.

an external $(2k-1, 2)$ 5-brane and an external $(2k-1, -2)$ 5-brane. The parts surrounded by the dashed circles need to be properly resolved and it introduces $k - 1$ faces for each part. Then the dimension of the Coulomb branch moduli space of the $5d$ theory can be counted by the number of faces in the diagram and it is

$$\dim \mathcal{M}_C = 2k + 1 + 2 + 2(k - 1) = 4k + 1. \tag{C.1}$$

At the infinitely strong coupling the diagram becomes the one in figure 45. The brane web
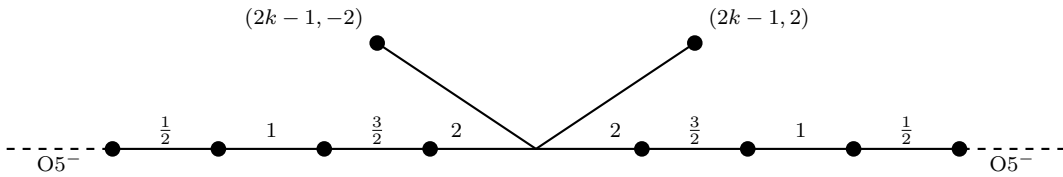
Figure 45: The orientifold web diagram for the theory given in Figure 44 at the infinitely strong coupling.

has $(2k-1, 2)$ 5-brane and the number of the charge 2 hypermultiplets coupled to the U(1) gauge node originated from the 5-brane is

$$\frac{8k - 4}{2} - 2 = 4k - 4 \tag{C.2}$$

according to (2.6). Namely the orientifold web diagram in figure 45 yields the orthosymplectic magnetic quiver depicted in (C.3).

$$\text{(C.3)}$$
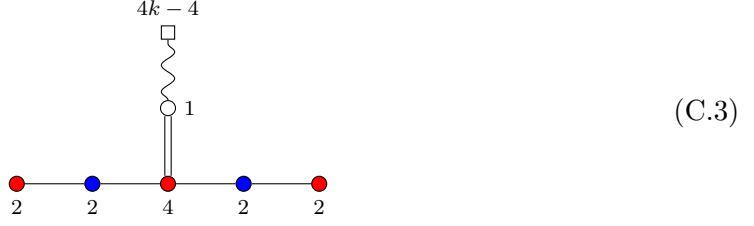
For counting the dimension of the Higgs branch moduli space of the theory in (C.3), we compute the number of hypermultiplets and the number of vector multiplets and then do subtraction. The number of hypermultipltes is

$$H = 2 + 4 + 4 + 2 + 8 + 4k - 4 = 16 + 4k, \tag{C.4}$$

and the number of vector multiplets is

$$V = 1 + 3 + 6 + 3 + 1 + 1 = 15. \tag{C.5}$$

Hence the dimension of the Higgs branch is given by

$$\dim \mathcal{M}_H = 16 + 4k - 15 = 4k + 1. \tag{C.6}$$

We find that (C.6) is exactly the same as (C.1) and this gives support for the number of charge 2 hypermultiplets counting in (C.2).

The first example is in the class of O5$^-$ - O5$^-$ and let us also consider an example in the class of O5$^+$ - O5$^+$. The second example we choose is the 5d theory realized on the 5-brane web diagram in figure 46. The central gauge theory is now an SO($12k + 2$)
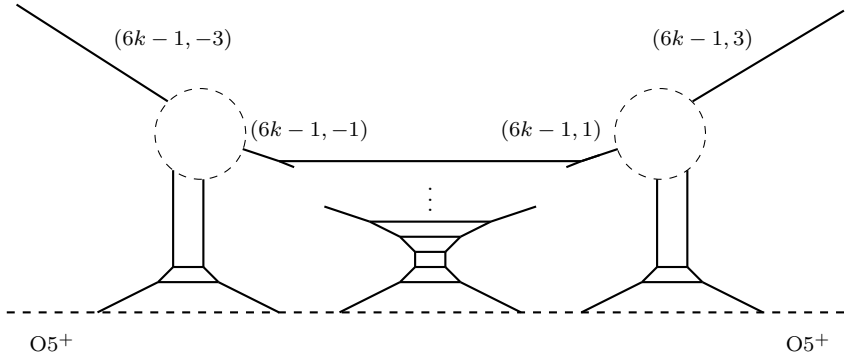
Figure 46: The 5-brane web diagram which has an external $(6k - 1, 3)$ 5-brane and an external $(6k - 1, -3)$ 5-brane.

gauge theory and the diagram contains an external $(6k - 1, 3)$ 5-brane and an external $(6k - 1, -3)$ 5-brane. The parts surrounded by the dashed circles again need to be resolved

and each part in fact has $6k - 2$ faces. In this case the dimension of the Coulomb branch moduli space of the 5d theory is

$$\dim\mathcal{M}_C = 6k + 1 + 2 + 6 + 2(6k - 2) = 18k + 5. \tag{C.7}$$

For reading off the magnetic quiver theory we take the infinitely strong coupling limit of the diagram in figure 46 and it becomes the one in figure 47. The $(6k-1, 3)$ 5-brane and the
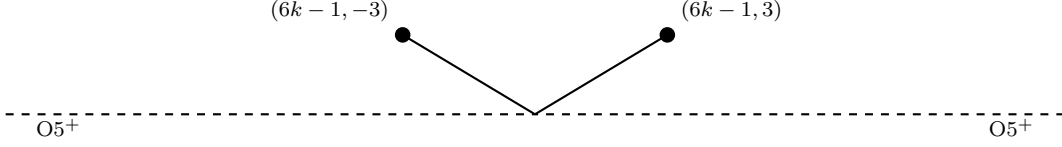
Figure 47: The orientifold web diagram for the theory given in Figure 46 at the infinitely strong coupling.

$(6k-1, -3)$ 5-brane yields a U(1) gauge theory and the number of charge 2 hypermultiplets computed by (3.5) is

$$\frac{6(3k - 1)}{2} - 3 = 18k - 6. \tag{C.8}$$

Furthermore we also expect the presence of the $3 \times 4 = 12$ charge 1 hypermutiplets which is computed by using (3.6). Then the magentic quiver theory which arises from the diagram in figure 47 is given in (C.9).

$$\tag{C.9}$$

We can compute the dimension of the Higgs branch moduli space of the orthosymplectic magnetic quiver theory in (C.9) in a similar way. The number of hypermulitplets in the quiver is

$$H = 18k - 6 + 12 = 18k + 6, \tag{C.10}$$

and the number of vector multiplets is

$$V = 1, \tag{C.11}$$

which yields

$$\dim\mathcal{M}_H = 18k + 5. \tag{C.12}$$

We again find the agreement with (C.7) which gives another support for (2.6).

D The remaining theories in the Y_N family

There are a few more possible configurations in the $Y_N^{p,q}$ family. They do not give rise to any new rules, in addition to those already mentioned so far. They do however serve as working examples, that demonstrate the validity of the rules proposed earlier. Without delving into a technical discussion, we present the web diagrams along with the corresponding magnetic quivers for the $Y_N^{p,q}$ family. We have also checked the matching of the Coulomb branch Hilbert series for the unitary and orthosymplectic quivers for each of the family. These results have been presented in various figures and tables, as summarized in the following.

Theory	Unitray web	Orientifold web	Magnetic quivers	Coulomb branch HS
$Y_N^{2,1}$	Figure 48	Figure 49	Table 19	Table 20
$Y_N^{3,1}$	Figure 50	Figure 51	Figure 52	Table 21
$Y_N^{2,2}$	Figure 53	Figure 54	Table 22	Table 23
$Y_N^{2,3}$	Figure 55	Figure 56	Figure 57	Table 24
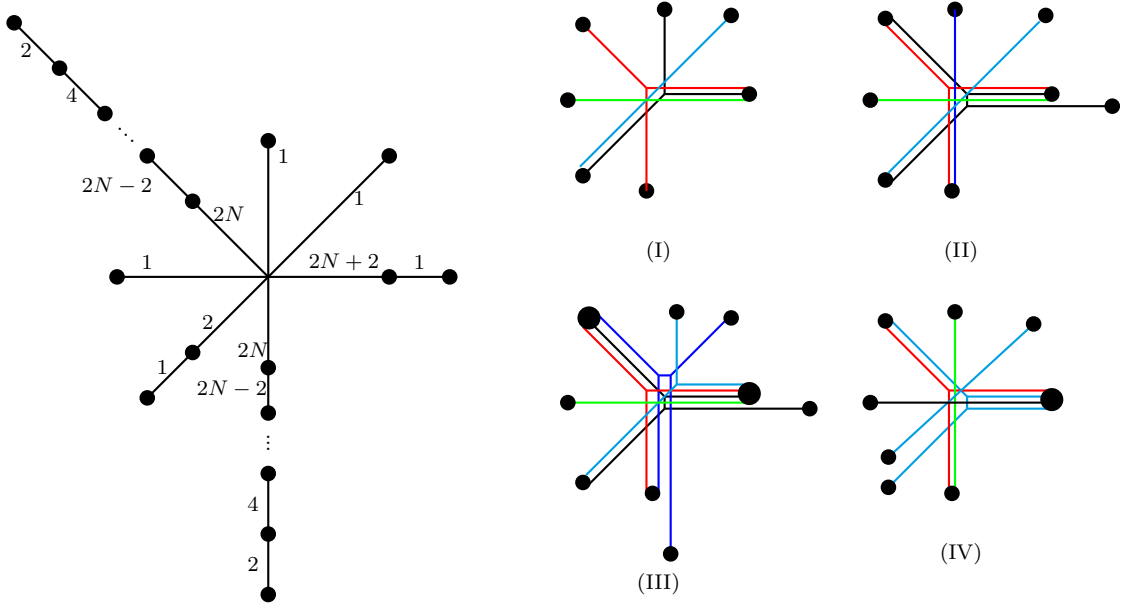
Figure 48: Ordinary web for the $Y_N^{2,1}$ theory along with its maximal subdivisions.
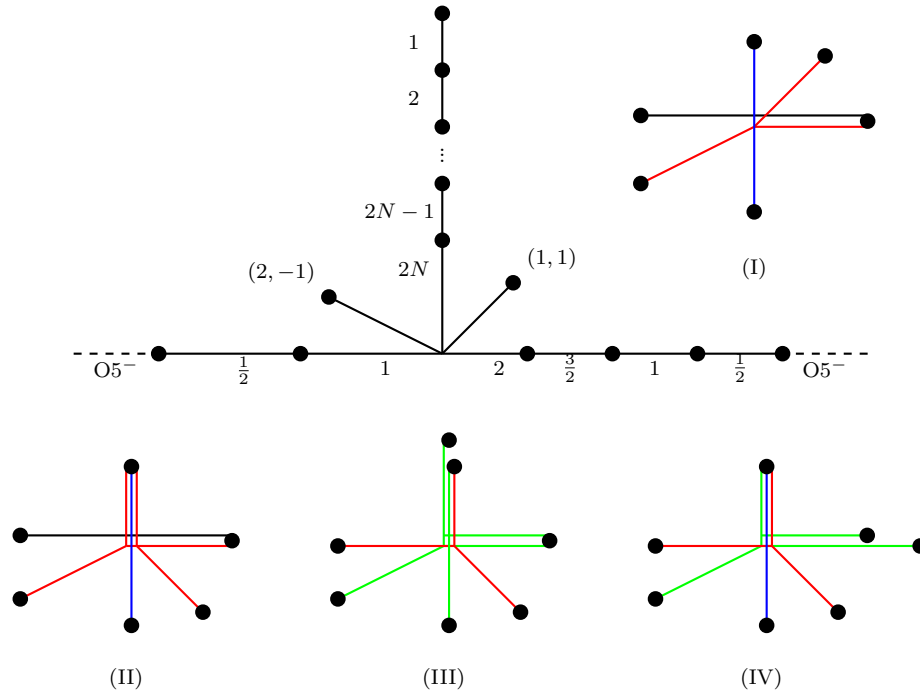
Figure 49: Orientifold web for the $Y_N^{2,1}$ theory along with its maximal subdivisions.
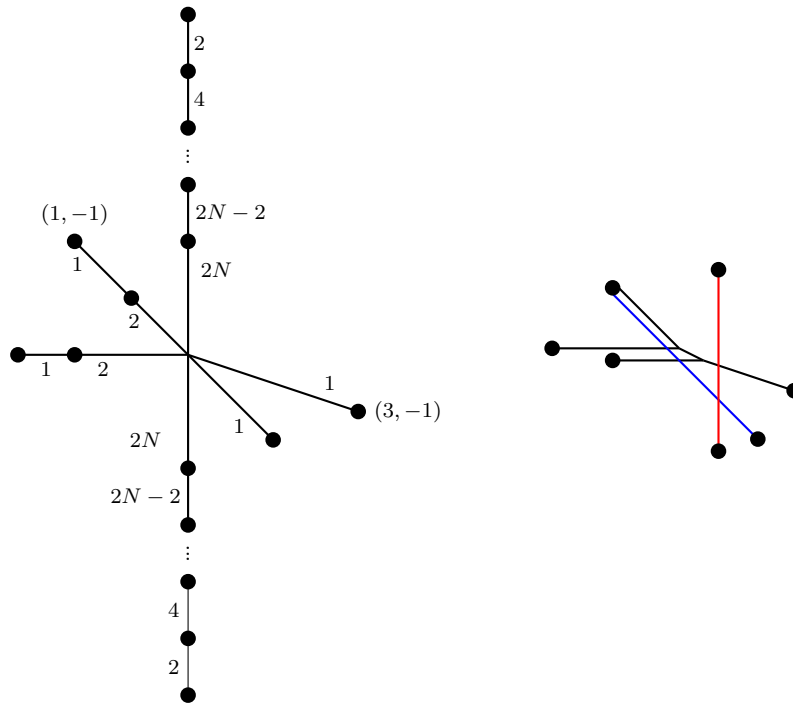
Figure 50: Ordinary web diagram for the $Y_N^{3,1}$ theory along with the maximal subdivision for the centre of the junction.

Table 19: The magnetic quivers derived from various maximal subdivisions (MS) of the unitary and orientifold webs of the $Y_N^{2,1}$ theory.
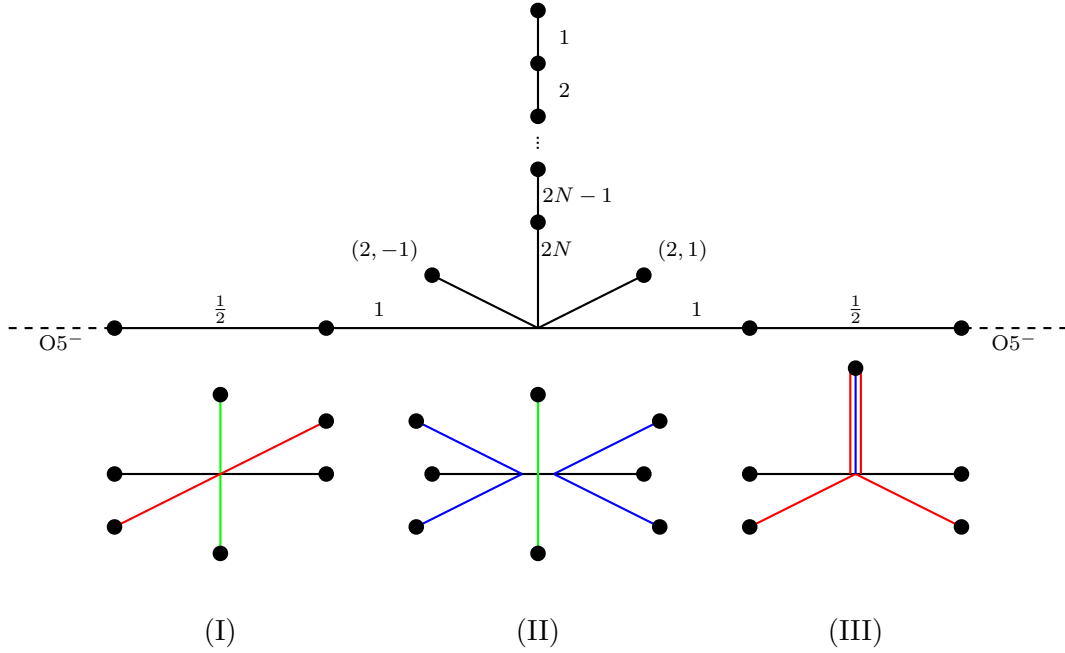
MS	Unitary	Orthosymplectic	
	$HS(t)$	$HS(t; \vec{m} \in \mathbb{Z})$	$HS(t; \vec{m} \in \mathbb{Z} + \frac{1}{2})$
$(I)_{N=1}$	$1 + 11t + 91t^2 + 552t^3 +$ $2654t^4 + 10598t^5 + \cdots$	$1 + 11t + 75t^2 + 392t^3 +$ $1710t^4 + 6422t^5 + \cdots$	$16t^2 + 160t^3 + 944t^4 +$ $4176t^5 + \cdots$
$(I)_{N=2}$	$1 + 23t + 289t^2 + 2638t^3 +$ $19566t^4 + 124453t^5 + \cdots$	$1 + 23t + 289t^2 + 2590t^3 +$ $18510t^4 + 111893t^5 + \cdots$	$48t^3 + 1056t^4 + 12560t^5 + \cdots$
$(II)_{N=1}$	$1 + 11t + 79t^2 + 405t^3 +$ $1644t^4 + 5572t^5 + \cdots$	$1 + 11t + 71t^2 + 325t^3 +$ $1196t^4 + 3764t^5 + \cdots$	$8t^2 + 80t^3 + 448t^4 +$ $1808t^5 + \cdots$
$(II)_{N=2}$	$1 + 23t + 289t^2 + 2622t^3 +$ $19178t^4 + 119256t^5 + \cdots$	$1 + 23t + 289t^2 + 2590t^3 +$ $18474t^4 + 110936t^5 + \cdots$	$32t^3 + 704t^4 + 8320t^5 + \cdots$
$(III)_{N=2}$	$1 + 23t + 273t^2 + 2255t^3 +$ $14595t^4 + 78621t^5 + \cdots$	$1 + 23t + 273t^2 + 2215t^3 +$ $13795t^4 + 70381t^5 + \cdots$	$40t^3 + 800t^4 + 8240t^5 + \cdots$
$(III)_{N=3}$	xx	xx	xx
$(IV)_{N=1}$	$1 + 8t + 46t^2 + 184t^3 +$ $599t^4 + 1648t^5 + \cdots$	$1 + 8t + 34t^2 + 108t^3 +$ $323t^4 + 872t^5 + \cdots$	$12t^2 + 76t^3 + 276t^4 +$ $776t^5 + \cdots$
$(IV)_{N=2}$	$1 + 20t + 224t^2 + 1843t^3 +$ $12276t^4 + 69526t^5 + \cdots$	$1 + 20t + 224t^2 + 1803t^3 +$ $11516t^4 + 61590t^5 + \cdots$	$40t^3 + 760t^4 + 7936t^5 + \cdots$

Table 20: Coulomb branch Hilbert series for the magnetic quivers of the $Y_N^{2,1}$ theory. The corresponding unitary and orthosymplectic quivers are given in table 19.
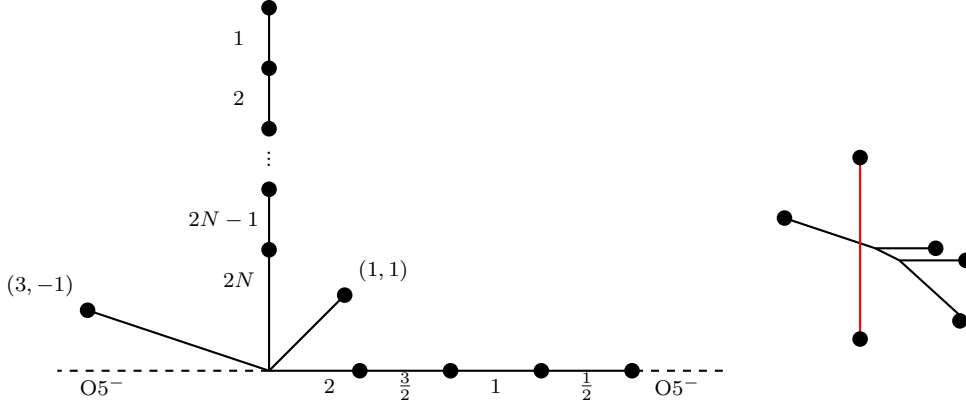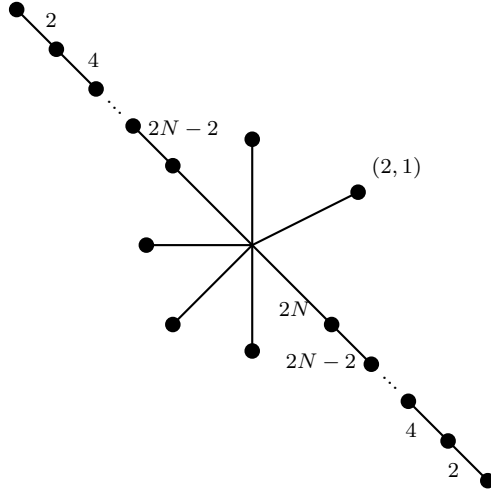

Figure 51: Orientifold web for the $Y_N^{3,1}$ theory along with the maximal subdivision at the centre of the junction.

(a) Orthosymplectic quiver
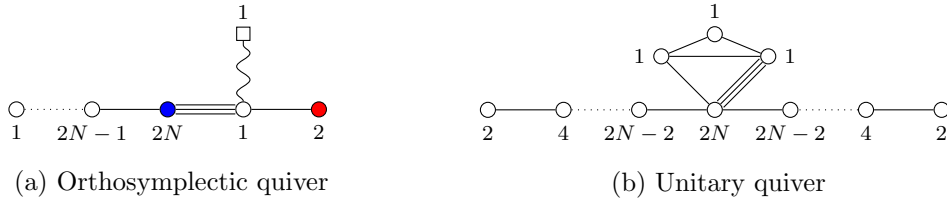
(b) Unitary quiver

Figure 52: The magnetic quivers for the $Y_N^{3,1}$ theory.

Theory	Unitary	Orthosymplectic	
	$\mathrm{HS}(t)$	$\mathrm{HS}(t; \vec{m} \in \mathbb{Z})$	$\mathrm{HS}(t; \vec{m} \in \mathbb{Z} + \frac{1}{2})$
$Y_1^{3,1}$	$1 + 7t + 38t^2 + 145t^3 + 463t^4 + 1252t^5 + \cdots$	$1 + 7t + 30t^2 + 97t^3 + 279t^4 + 716t^5 + \cdots$	$8t^2 + 48t^3 + 184t^4 + 536t^5 + \cdots$
$Y_2^{3,1}$	$1 + 19t + 204t^2 + 1603t^3 + 10173t^4 + 54879t^5 + \cdots$	$1 + 19t + 204t^2 + 1579t^3 + 9741t^4 + 50543t^5 + \cdots$	$24t^3 + 432t^4 + 4336t^5 + \cdots$

Table 21: Coulomb branch Hilbert series for the magnetic quivers in the figure 52 for the $Y_N^{3,1}$ theory.
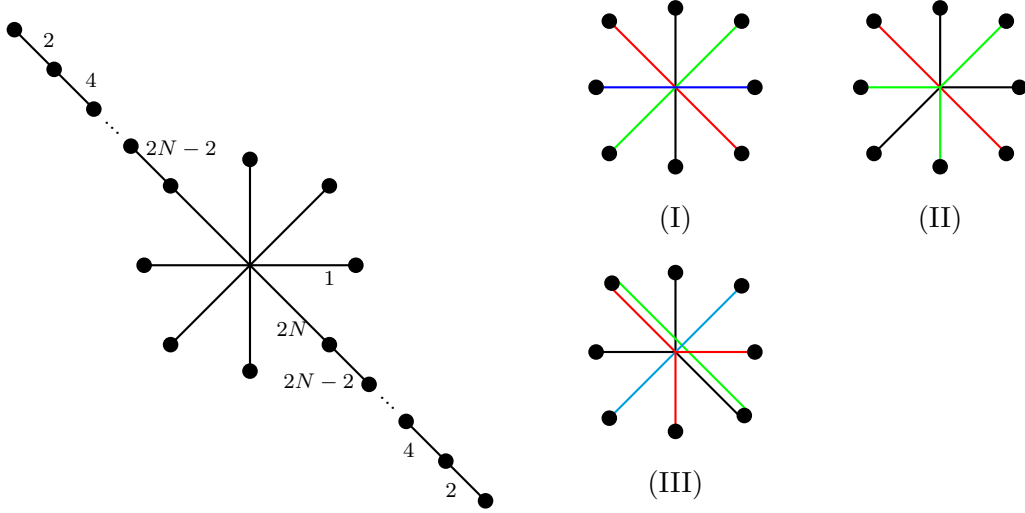
Figure 53: Ordinary web for the $Y_N^{2,2}$ theory at the fixed point, along with the possible maximal subdivisions of the centre of the junction.

Table 22: The magnetic quivers derived from the various maximal subdivisions (MS) of the unitary and orientifold web diagrams of the $Y_N^{2,2}$ theory.

Figure 54: Orientifold web for the $Y_N^{2,2}$ theory along with its maximal subdivisions. In the subdivision marked as (II), the blue and red subweb are related to the discrete theta angle from O5 plane and are thus immobile.

MS	Unitary	Orthosymplectic	
	$HS(t)$	$HS(t; \vec{m} \in \mathbb{Z})$	$HS(t; \vec{m} \in \mathbb{Z} + \frac{1}{2})$
$(I)_{N=1}$	$1 + 5t + 28t^2 + 105t^3 +$ $339t^4 + 920t^5 + \cdots$	$1 + 5t + 20t^2 + 65t^3 +$ $195t^4 + 512t^5 + \cdots$	$8t^2 + 40t^3 + 144t^4 +$ $408t^5 + \cdots$
$(I)_{N=2}$	$1 + 17t + 168t^2 + 1233t^3 +$ $7427t^4 + 38575t^5 + \cdots$	$1 + 17t + 168t^2 + 1209t^3 +$ $7019t^4 + 34671t^5 + \cdots$	$24t^3 + 408t^4 + 3904t^5 + \cdots$
$(II)_{N=1}$	$1 + 4t + 15t^2 + 45t^3 +$ $110t^4 + 239t^5 + \cdots$	$1 + 4t + 15t^2 + 45t^3 +$ $110t^4 + 239t^5 + \cdots$	not required
$(II)_{N=2}$	$1 + 16t + 151t^2 + 1041t^3 +$ $5810t^4 + 27652t^5 + \cdots$	$1 + 16t + 151t^2 + 1041t^3 +$ $5810t^4 + 27652t^5 + \cdots$	not required
$(III)_{N=1}$	$1 + 5t + 20t^2 + 60t^3 +$ $151t^4 + 331t^5 + \cdots$	$1 + 5t + 16t^2 + 40t^3 +$ $91t^4 + 191t^5 + \cdots$	$4t^2 + 20t^3 + 60t^4 + 140t^5 + \cdots$
$(III)_{N=2}$	$1 + 17t + 168t^2 + 1225t^3 +$ $7255t^4 + 36626t^5 + \cdots$	$1 + 17t + 168t^2 + 1209t^3 +$ $6983t^4 + 34050t^5 + \cdots$	$16t^3 + 272t^4 + 2576t^5 + \cdots$

Table 23: Coulomb branch Hilbert series for magnetic quivers of the $Y_N^{2,2}$ theory. The corresponding unitary and orthosymplectic quivers are given in table 22.

Figure 55: Unitary web description of the $Y_N^{2,3}$ theory.
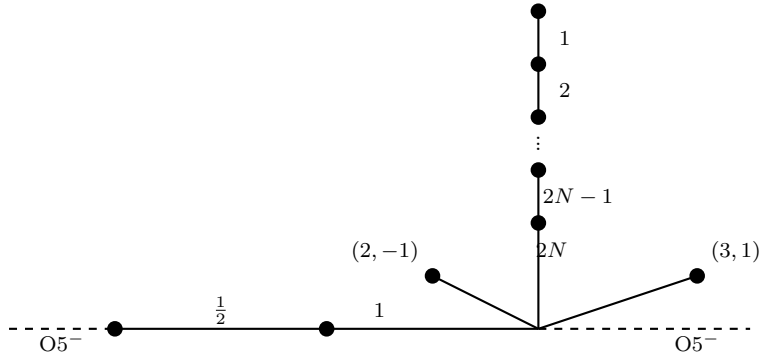
Figure 56: Orientifold web description of the $Y_N^{2,3}$ theory.

(a) Orthosymplectic quiver
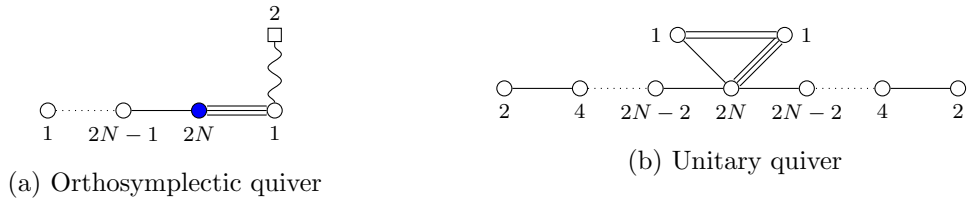
(b) Unitary quiver

Figure 57: The magnetic quivers for the $Y_N^{2,3}$ theory.

Theory	Unitary	Orthosymplectic	
	HS(t)	HS($t; \vec{m} \in \mathbb{Z}$)	HS($t; \vec{m} \in \mathbb{Z} + \frac{1}{2}$)
$Y_1^{2,3}$	$1 + 4t + 17t^2 + 47t^3 +$ $120t^4 + 255t^5 + \cdots$	$1 + 4t + 13t^2 + 31t^3 +$ $72t^4 + 147t^5 + \cdots$	$4t^2 + 16t^3 + 48t^4 + 108t^5 + \cdots$
$Y_2^{2,3}$	$1 + 16t + 151t^2 + 1051t^3 +$ $5940t^4 + 28640t^5 + \cdots$	$1 + 16t + 151t^2 + 1039t^3 +$ $5748t^4 + 26892t^5 + \cdots$	$12t^3 + 192t^4 + 1748t^5 + \cdots$

Table 24: Coulomb branch Hilbert series for the magnetic quivers in the figure 57 for the $Y_N^{2,3}$ theory.

List of Figures

List of Tables

References

[1] A. Bourget, J. F. Grimminger, A. Hanany, M. Sperling, and Z. Zhong, *Magnetic Quivers from Brane Webs with O5 Planes*, arXiv:2004.04082.

[2] N. Seiberg, *Five-dimensional SUSY field theories, nontrivial fixed points and string dynamics*, *Phys.Lett.* **B388** (1996) 753–760, [[hep-th/9608111](hep-th/9608111)].

[3] K. A. Intriligator, D. R. Morrison, and N. Seiberg, *Five-dimensional supersymmetric gauge theories and degenerations of Calabi-Yau spaces*, *Nucl.Phys.* **B497** (1997) 56–100, [[hep-th/9702198](hep-th/9702198)].

[4] D. R. Morrison and N. Seiberg, *Extremal transitions and five-dimensional supersymmetric field theories*, *Nucl.Phys.* **B483** (1997) 229–247, [[hep-th/9609070](hep-th/9609070)].

[5] H.-C. Kim, S.-S. Kim, and K. Lee, *5-dim Superconformal Index with Enhanced En Global Symmetry*, *JHEP* **1210** (2012) 142, [arXiv:1206.6781].

[6] D. Bashkirov, *A comment on the enhancement of global symmetries in superconformal SU(2) gauge theories in 5D*, arXiv:1211.4886.

[7] A. Iqbal and C. Vafa, *BPS Degeneracies and Superconformal Index in Diverse Dimensions*, *Phys.Rev.* **D90** (2014), no. 10 105031, [arXiv:1210.3605].

[8] D. Rodríguez-Gómez and G. Zafrir, *On the 5d instanton index as a Hilbert series*, *Nucl. Phys. B* **878** (2014) 1–11, [arXiv:1305.5684].

[9] M. Taki, *Notes on Enhancement of Flavor Symmetry and 5d Superconformal Index*, arXiv:1310.7509.

[10] O. Bergman, D. Rodríguez-Gómez, and G. Zafrir, *Discrete θ and the 5d superconformal index*, *JHEP* **1401** (2014) 079, [arXiv:1310.2150].

[11] O. Bergman, D. Rodríguez-Gómez, and G. Zafrir, *5-Brane Webs, Symmetry Enhancement, and Duality in 5d Supersymmetric Gauge Theory*, *JHEP* **03** (2014) 112, [arXiv:1311.4199].

[12] O. Bergman and G. Zafrir, *Lifting 4d dualities to 5d*, *JHEP* **1504** (2015) 141, [arXiv:1410.2806].

[13] C. Hwang, J. Kim, S. Kim, and J. Park, *General instanton counting and 5d SCFT*, *JHEP* **07** (2015) 063, [arXiv:1406.6793]. [Addendum: JHEP04,094(2016)].

[14] G. Zafrir, *Duality and enhancement of symmetry in 5d gauge theories*, *JHEP* **12** (2014) 116, [arXiv:1408.4040].

[15] L. Bao, V. Mitev, E. Pomoni, M. Taki, and F. Yagi, *Non-Lagrangian Theories from Brane Junctions*, *JHEP* **1401** (2014) 175, [arXiv:1310.3841].

[16] S.-S. Kim, M. Taki, and F. Yagi, *Tao Probing the End of the World*, *PTEP* **2015** (2015), no. 8 083B02, [arXiv:1504.03672].

[17] H. Hayashi, H.-C. Kim, and T. Nishinaka, *Topological strings and 5d T_N partition functions*, *JHEP* **1406** (2014) 014, [arXiv:1310.3854].

[18] V. Mitev, E. Pomoni, M. Taki, and F. Yagi, *Fiber-Base Duality and Global Symmetry Enhancement*, *JHEP* **1504** (2015) 052, [arXiv:1411.2450].

[19] S.-S. Kim and F. Yagi, *5d E_n Seiberg-Witten curve via toric-like diagram*, *JHEP* **06** (2015) 082, [arXiv:1411.7903].

[20] H. Hayashi and G. Zoccarato, *Topological vertex for Higgsed 5d T_N theories*, JHEP **09** (2015) 023, [arXiv:1505.00260].

[21] H. Hayashi, S.-S. Kim, K. Lee, M. Taki, and F. Yagi, *A new 5d description of 6d D-type minimal conformal matter*, JHEP **08** (2015) 097, [arXiv:1505.04439].

[22] H. Hayashi, S.-S. Kim, K. Lee, and F. Yagi, *Discrete theta angle from an O5-plane*, JHEP **11** (2017) 041, [arXiv:1707.07181].

[23] H. Hayashi, S.-S. Kim, K. Lee, and F. Yagi, *Dualities and 5-brane webs for 5d rank 2 SCFTs*, JHEP **12** (2018) 016, [arXiv:1806.10569].

[24] H. Hayashi, S.-S. Kim, K. Lee, and F. Yagi, *Complete prepotential for 5d $\mathcal{N} = 1$ superconformal field theories*, JHEP **02** (2020) 074, [arXiv:1912.10301].

[25] N. Lambert, C. Papageorgakis, and M. Schmidt-Sommerfeld, *Instanton Operators in Five-Dimensional Gauge Theories*, JHEP **03** (2015) 019, [arXiv:1412.2789].

[26] D. Rodriguez-Gomez and J. Schmude, *Supersymmetrizing 5d instanton operators*, JHEP **03** (2015) 114, [arXiv:1501.00927].

[27] Y. Tachikawa, *Instanton operators and symmetry enhancement in 5d supersymmetric gauge theories*, PTEP **2015** (2015), no. 4 043B06, [arXiv:1501.01031].

[28] G. Zafir, *Instanton operators and symmetry enhancement in 5d supersymmetric USp, SO and exceptional gauge theories*, JHEP **07** (2015) 087, [arXiv:1503.08136].

[29] K. Yonekura, *Instanton operators and symmetry enhancement in 5d supersymmetric quiver gauge theories*, JHEP **07** (2015) 167, [arXiv:1505.04743].

[30] O. Aharony and A. Hanany, *Branes, superpotentials and superconformal fixed points*, Nucl.Phys. **B504** (1997) 239–271, [hep-th/9704170].

[31] O. Aharony, A. Hanany, and B. Kol, *Webs of (p,q) five-branes, five-dimensional field theories and grid diagrams*, JHEP **9801** (1998) 002, [hep-th/9710116].

[32] O. DeWolfe, A. Hanany, A. Iqbal, and E. Katz, *Five-branes, seven-branes and five-dimensional E(n) field theories*, JHEP **03** (1999) 006, [hep-th/9902179].

[33] M. R. Gaberdiel and B. Zwiebach, *Exceptional groups from open strings*, Nucl.Phys. **B518** (1998) 151–172, [hep-th/9709013].

[34] M. R. Gaberdiel, T. Hauer, and B. Zwiebach, *Open string-string junction transitions*, Nucl.Phys. **B525** (1998) 117–145, [hep-th/9801205].

[35] D. Gaiotto and H.-C. Kim, *Duality walls and defects in 5d $\mathcal{N} = 1$ theories*, JHEP **01** (2017) 019, [arXiv:1506.03871].

[36] G. Zafir, *Brane webs, 5d gauge theories and 6d $\mathcal{N} = (1, 0)$ SCFT's*, JHEP **12** (2015) 157, [arXiv:1509.02016].

[37] H. Hayashi, S.-S. Kim, K. Lee, and F. Yagi, *6d SCFTs, 5d Dualities and Tao Web Diagrams*, JHEP **05** (2019) 203, [arXiv:1509.03300].

[38] H. Hayashi, S.-S. Kim, K. Lee, M. Taki, and F. Yagi, *More on 5d descriptions of 6d SCFTs*, JHEP **10** (2016) 126, [arXiv:1512.08239].

[39] P. Jefferson, S. Katz, H.-C. Kim, and C. Vafa, *On Geometric Classification of 5d SCFTs*, JHEP **04** (2018) 103, [arXiv:1801.04036].

[40] S. Cremonesi, G. Ferlito, A. Hanany, and N. Mekareeya, *Instanton Operators and the Higgs Branch at Infinite Coupling*, *JHEP* **04** (2017) 042, [arXiv:1505.06302].

[41] G. Ferlito, A. Hanany, N. Mekareeya, and G. Zafir, *3d Coulomb branch and 5d Higgs branch at infinite coupling*, *JHEP* **07** (2018) 061, [arXiv:1712.06604].

[42] F. Benini, S. Benvenuti, and Y. Tachikawa, *Webs of five-branes and N=2 superconformal field theories*, *JHEP* **0909** (2009) 052, [arXiv:0906.0359].

[43] F. Benini, Y. Tachikawa, and D. Xie, *Mirrors of 3d Sicilian theories*, *JHEP* **09** (2010) 063, [arXiv:1007.0992].

[44] J. Eckhard, S. Schafer-Nameki, and Y.-N. Wang, *Trifectas for T_N in 5d*, *JHEP* **07** (2020) 199, [arXiv:2004.15007].

[45] S. Cabrera, A. Hanany, and F. Yagi, *Tropical Geometry and Five Dimensional Higgs Branches at Infinite Coupling*, *JHEP* **01** (2019) 068, [arXiv:1810.01379].

[46] S. Cabrera, A. Hanany, and M. Sperling, *Magnetic quivers, Higgs branches, and 6d N=(1,0) theories*, *JHEP* **06** (2019) 071, [arXiv:1904.12293]. [Erratum: JHEP 07, 137 (2019)].

[47] O. Bergman, D. Rodríguez-Gómez, and C. F. Uhlemann, *Testing AdS_6/CFT_5 in Type IIB with stringy operators*, *JHEP* **08** (2018) 127, [arXiv:1806.07898].

[48] G. Zafir, *Brane webs in the presence of an $O5^-$-plane and 4d class S theories of type D*, *JHEP* **07** (2016) 035, [arXiv:1602.00130].

[49] D. Gaiotto and E. Witten, *S-Duality of Boundary Conditions In N=4 Super Yang-Mills Theory*, *Adv. Theor. Math. Phys.* **13** (2009), no. 3 721–896, [arXiv:0807.3720].

[50] Z. Zhong, *Quiver gauge theories in 3d, 5d and 6d*, Master's thesis, Imperial College, London,, 2018.

[51] A. Bourget, J. F. Grimminger, A. Hanany, R. Kalveks, M. Sperling, and Z. Zhong, *Magnetic Lattices for Orthosymplectic Quivers*, arXiv:2007.04667.

[52] M. van Beest, A. Bourget, J. Eckhard, and S. Schafer-Nameki, *(Symplectic) Leaves and (5d Higgs) Branches in the Poly(go)nesian Tropical Rain Forest*, arXiv:2008.05577.

[53] O. Bergman and G. Zafir, *5d fixed points from brane webs and O7-planes*, *JHEP* **12** (2015) 163, [arXiv:1507.03860].

[54] M. Akhond, F. Carta, S. Dwivedi, H. Hayashi, S.-S. Kim, and F. Yagi, *Work in progress*, .

[55] A. Bourget, J. F. Grimminger, A. Hanany, M. Sperling, G. Zafir, and Z. Zhong, *Magnetic quivers for rank 1 theories*, arXiv:2006.16994.

[56] C. Closset, S. Schafer-Nameki, and Y.-N. Wang, *Coulomb and Higgs Branches from Canonical Singularities: Part 0*, arXiv:2007.15600.

[57] S. Cremonesi, A. Hanany, and A. Zaffaroni, *Monopole operators and Hilbert series of Coulomb branches of 3d $\mathcal{N} = 4$ gauge theories*, *JHEP* **01** (2014) 005, [arXiv:1309.2657].